A STUDY OF NEUTRON-CAPTURE GAMMA-RAY SPECTRA FROM ALIGNED NEODYMIUM AND SAMARIUM NUCLEI

E.R.REDDINGIUS

A STUDY OF NEUTRON-CAPTURE GAMMA-RAY SPECTRA FROM ALIGNED NEODYMIUM AND SAMARIUM NUCLEI

STELLINGEN

1. De veronderstelling van Matvienko en medewerkers, dat de door hen waargenomen temperatuurafhankelijkheid van de hoekverdeling van de door gerichte ^{233}U-kernen uitgezonden α-deeltjes kan worden verklaard door een grote konstante voor de magnetische hyperfijnsplitsing in de spin-Hamiltoniaan is in tegenspraak met het beeld dat Eisenstein en Price geven voor het $(UO_2)^{2+}$-ion.

   V.I.Matvienko e.a., Soviet J. Nucl. Phys. 7(1968)297.

   J.C.Eisenstein en M.H.L.Price, Proc. Roy. Soc. (London) A229 (1955)20.

2. Voor het langdurig in stand houden van een goed vacuum in een cryostaat van een Ge(Li)-detector heeft het gebruik van een aparte zeolietpomp, welke losgekoppeld en onder verwarming leeggepompt kan worden, voordelen boven het gebruik van zeoliet in de cryostaat zelf.

3. Tegen de door Zehender en Fleischmann gegeven interpretatie van de door hen met behulp van de som-coincidentiemethode waargenomen neutronvangst-gammaspectra van ^{143}Nd-kernen zijn bezwaren aan te voeren.

   O.Zehender en R.Fleischmann, Zeitschr. Phys. 188(1965)93.

4. Bij het samenstellen van het vervalschema van ^{140}Ce hebben El-Nesr en El-Aassar geen rekening gehouden met het feit dat in even-even kernen energieniveaus met een energie lager dan de paarenergie een collectief karakter hebben.

   M.S.El-Nesr en M.R.El-Aassar, Zeitschr. Naturforsch. 22a(1967) 299.

5. De door O'Brien aangegeven methode voor de bepaling van de konstanten van de associatie- en dissociatiesnelheid van een enzym-substraat complex is principieel onmogelijk.

   R.D.O'Brien, Mol. Pharmacol. 4(1968)121.

6. Vooral indien neutronresonanties met verschillende spin bijdragen tot de vangst in het thermische gebied, verdient het aanbeveling experimenten,

zoals beschreven in dit proefschrift, uit te voeren bij de neutronenergieën van verschillende resonanties.

7. Tegen het door Loere en medewerkers voorgestelde vervalschema van ^{150}Sm, waarbij drie 'rotatie' banden op aangeslagen 0^+ niveaus worden aangegeven, zijn bezwaren aan te voeren.

   E.Ya.Loere e.a., Isvestia Akademii Nauk SSSR serie Phys. XXXII (1968)74.

8. De continue en relatief grote koelcapaciteit van ^3He-^4He koelmachines maken experimenten met georienteerde kernen bij versnellers beter uitvoerbaar.

9. Tegen de door Voss en Matsumura gegeven beoordeling van de betekenis van hun proeven over de remming van acetylcholinesterase door een fosforester in aanwezigheid van acetylcholine zijn bezwaren aan te voeren.

   G.Voss en F.Matsumura, Nature 202(1964)319.

10. Indien, zoals voorgesteld in de nota-Posthumus, de normale tijd nodig voor een doctoraal studie in de natuurkunde wordt verkort tot vier jaar, zal men er rekening mee moeten houden dat op korte termijn de kennis en ervaring die gedurende de studie wordt opgedaan minder zal zijn dan voorheen het geval was.

18 juni 1969

E.R.Reddingius

RECEPTIE NA AFLOOP
DER PROMOTIE IN HET UNIVERSITEITSGEBOUW

E. R. Reddingius Weissenbruchstraat 12 Alkmaar

A STUDY OF NEUTRON-CAPTURE GAMMA-RAY SPECTRA FROM ALIGNED NEODYMIUM AND SAMARIUM NUCLEI

PROEFSCHRIFT

TER VERKRIJGING VAN DE GRAAD VAN DOCTOR IN
DE WISKUNDE EN NATUURWETENSCHAPPEN AAN DE
RIJKSUNIVERSITEIT TE LEIDEN OP GEZAG VAN
DE RECTOR MAGNIFICUS DR L. KUKENHEIM Ezn,
HOOGLERAAR IN DE FACULTEIT DER LETTEREN
TEN OVERSTAAN VAN EEN COMMISSIE UIT DE
SENAAT TE VERDEDIGEN OP
WOENSDAG 18 JUNI 1969 TE KLOKKE 14.15 UUR

EWOUT ROELOF REDDINGIUS

GEBOREN TE BATAVIA, NED. INDIE IN 1934

1969
AVANTI - ZALTBOMMEL

PROMOTOR: PROF. DR C.J. GORTER
COREFERENT: PROF. DR H. DE WAARD

DIT PROEFSCHRIFT IS BEWERKT ONDER LEIDING VAN
DR. H. POSTMA.

AAN HANNIE

Het in dit proefschrift beschreven onderzoek werd uitgevoerd als onderdeel van het programma van de werkgroep K IV van de stichting voor Fundamenteel Onderzoek der Materie met financiële steun van de Nederlandse Organisatie voor Zuiver Wetenschappelijk Onderzoek.

CONTENTS

CHAPTER I

INTRODUCTION AND SURVEY

The properties of nuclear energy levels such as half-lives, spins and parities and the characteristics of transitions between the energy levels such as transition probabilities and multipole mixtures in the case of gamma transitions can be derived from many experiments. Most information is obtained from the decay of radioactive nuclei, from particle reactions and from Coulomb excitation. In the experiments which are described in this thesis use has been made of the (n,γ) reaction. After neutron capture the nucleus is in a highly excited state which is about five to eight MeV above the ground state. In most cases the compound nucleus decays by the emission of gamma rays. The number of nuclear energy levels which can be studied is rather large since, especially for heavy nuclei, there are many possible cascades from the capturing state to the ground state with about three to six gamma's in each cascade. For thermal neutrons only s-wave neutron capture takes place. Thus the spin of the initial state of the compound nucleus is either $J=I+\frac{1}{2}$ or $J=I-\frac{1}{2}$ where I is the spin of the target nucleus. Often neutron capture at thermal energy is related to two or more resonances with different spin states for the compound nucleus and both values of J have to be taken into account. In general, energy levels having spins which are close to the spin of the capturing state can be studied. Decay schemes can be deduced from gamma-gamma coincidence and precise energy and intensity measurements. The spins and parities of the energy levels and the multipole mixtures of the gamma transitions are also of interest for a comparison with nuclear models. They are often derived from angular correlation or circular polarization measurements, from electron conversion coefficients or from gamma ray transition probabilities.

In this thesis experiments are described in which the spins and parities of energy levels and the multipole mixtures of the gamma transitions are determined by measuring the anisotropy in the directional distribution and

degree of linear polarization of neutron-capture gamma rays from oriented nuclei. Such experiments can be performed on nuclei which fulfil the following conditions:

a. The nuclei have a spin which is not equal to zero.
b. A suitable substance exists in which the nuclei can be oriented.
c. The nuclei have a sufficiently large capture cross-section for (thermal) neutrons.

The first condition restricts the experiments to odd-even, even-odd and a few odd-odd isotopes. It has been shown that condition b is fulfilled for several nuclei. The methods of nuclear orientation which make use of low temperature techniques are reviewed in detail in a number of articles[1-4] and will be discussed briefly. Nuclear orientation can be achieved at sufficiently low temperatures if a coupling is present between the nuclear magnetic dipole moment and a magnetic field or between the nuclear electric quadrupole moment and an inhomogeneous electric field. In principle it is possible to use an external magnetic field (brute force method). However, the degrees of nuclear orientation obtained in this way are insufficient for a measurement of the anisotropy and linear polarization of neutron-capture gamma rays. More successful are methods which make use of the strong internal magnetic fields which exist in paramagnetic ions. If a small magnetic field is used to polarize the paramagnetic ions a considerable nuclear orientation can be achieved. This method has been proposed by C.J.Gorter and M.E.Rose and is called the method of magnetic hyperfine structure polarization. Often the magnetic properties are anisotropic with respect to crystallographic axes. By cooling a single crystal with such properties to sufficiently low temperatures the ionic magnetic moments and consequently the nuclei will be oriented. It is known as the method of magnetic hyperfine structure alignment and has originally been proposed by B.Bleaney. In some crystals a strong coupling exists between the nuclear electric quadrupole moment and an electric field gradient at the nucleus. For some nuclei with large quadrupole deformations nuclear orientation has been obtained by cooling such crystals. This method has been proposed by R.V.Pound and is known as the method of electric hyperfine structure alignment. Nuclear orientation has also been obtained in ferromagnetic materials and anti-ferromagnetic single crystals. In all these so-called static methods mentioned above there is thermodynamic equilibrium between the nuclear spin system and the surrounding material. In another class

of methods transitions are introduced between the different magnetic substates by the aid of electromagnetic radiation. The equilibrium Boltzmann distribution is disturbed and depending on the detailed properties of the sample, considerable nuclear orientation can sometimes be obtained by these dynamic methods. In the latter methods it is often necessary to cool the sample to very low temperatures. For the static methods temperatures well below 0.1 K are usually necessary which can be obtained by adiabatic demagnetization or by the aid of a ^{3}He-^{4}He dilution refrigerator.

Condition c is related to the intensities of the observable gamma transitions and the abundances of the isotopes. In general there are several stable isotopes of the same element which may contribute to the neutron-capture gamma-ray spectrum. In principle the experiment can be performed with a sample enriched in one isotope. An alternative possibility is to study the capture gamma-ray spectra of isotopically enriched samples in an experiment separate from the alignment experiments. Also the influence of the other elements of which the sample is composed and of the surrounding material (cryostat, magnet, etc.) on the neutron-capture gamma-ray spectrum has to be considered. With the equipment at the high flux reactor in Petten in its present condition a cross-section for thermal neutrons of 10 barns will be sufficient in most cases although much depends on the conditions mentioned above. With samples which contain the oriented nuclei in a high concentration such as single crystals of metals, isotopes with a much lower cross-section can be studied.

The conditions given above are fulfilled for the nuclei ^{143}Nd and ^{149}Sm which can be aligned in single crystals of neodymium ethylsulphate and cerium (samarium) magnesium double nitrate, respectively, using Bleaney's method. The necessary low temperatures can be obtained by adiabatic demagnetization of these crystals.

In the first experiments with capture gamma rays from oriented nuclei the spectra were measured with NaI(Tl) detectors[5]. The efficiency of these detectors is rather high but their poor resolution is a disadvantage. Other detectors which have a much better resolution such as diffraction spectrometers and magnetic Compton spectrometers can not be used because they have a much too low efficiency. The Ge(Li) detectors which have been developed in the last few years are very suitable for capture gamma-ray spectroscopy. The resolution of these detectors is at least an order of magnitude better

than of NaI(Tl) detectors and for energies above 5 MeV they even have a better resolution than the existing magnetic Compton spectrometers[6]. Due to the development of better techniques of manufacturing these detectors and the necessary electronic equipment the resolution was much improved in the course of the experiments described in the next chapters.

In chapter II formulas are given which describe the dependence of the directional distribution and the degree of linear polarization of gamma rays on the spins and parities of the energy levels and the multipole mixtures in the transitions. Special attention is given to the disorientation due to neutron capture and the preceding gamma rays. The neutron beams, the cryostat, the magnet for the adiabatic demagnetizations, the detectors, the polarimeter and the electronic equipment are described in chapter III. The experimental results obtained for neodymium and samarium are given in chapter IV and V, respectively. The decay schemes of ^{144}Nd, ^{146}Nd, ^{150}Sm, ^{148}Sm and ^{153}Sm are discussed. Some general remarks concerning the energy level schemes of even-even nuclei are given in chapter VI.

REFERENCES

1. Steenland, M.J. and Tolhoek, H.A., Progress in Low Temperature Physics, Volume 2, Chapter X, edited by C.J.Gorter (North Holland Publ.Comp. Amsterdam 1957).
2. Huiskamp, W.J. and Tolhoek, H.A., Progress in Low Temperature Physics, Volume 3, Chapter VIII, edited by C.J.Gorter (North Holland Publ.Comp. Amsterdam 1961).
3. De Groot, S.R., Tolhoek, H.A. and Huiskamp, W.J., Alpha-, Beta- and Gamma-Ray Spectroscopy, Volume 2, Chapter XIXB, edited by K.Siegbahn. (North Holland Publ. Comp. Amsterdam 1965).
4. Shirley, D.A., Annual Review of Nuclear Science 16 (1966) 89.
5. Postma, H. and Reddingius, E.R., Physica 34 (1967) 541.
6. Motz, H. and Bäckström, G., Alpha-, Beta- and Gamma-Ray Spectroscopy, Volume 1, Chapter XIII, edited by K.Siegbahn. (North Holland Publ.Comp. Amsterdam 1965).

CHAPTER II

DIRECTIONAL DISTRIBUTION AND LINEAR POLARIZATION OF NEUTRON-CAPTURE GAMMA RAYS FROM ALIGNED NUCLEI

If we restrict ourselves to systems with an axis of rotational symmetry the degree of nuclear orientation can be described by the parameters f_k, which have originally been defined by Tolhoek and Cox[1]. Denoting the probability of finding the nucleus with spin I in the substate $m \equiv I_z$, where z is the axis of rotational symmetry, by a_m the orientation parameters are given by the following expression:

$$f_k(I) = \binom{2k}{k}^{-1} I^{-k} \sum_m \sum_{\nu=0}^{k} (-1)^{\nu} \frac{(I-m)!\,(I+m)!}{(I-m-\nu)!\,(I+m-k+\nu)!} \binom{k}{\nu}^2 a_m. \qquad 2.1$$

They are identically zero for all $k > 2I$. Explicit formulas for the orientation parameters f_1, f_2, f_3 and f_4 can be found in ref. 1. The nuclei are said to be aligned if $a_m = a_{-m}$ for all m. In that case all f_k with k odd are zero. If $a_m \neq a_{-m}$ for at least one value of m the f_k with k odd are in general not zero and the nuclei are said to be polarized. The axis of rotational symmetry will henceforth also be called the axis of nuclear orientation or of nuclear alignment.

The directional distribution of gamma rays from oriented nuclei can be written as follows[1]:

$$W(\theta) = 1 + \sum_{k=\text{even}} f_k G_k A_k P_k(\cos\theta). \qquad 2.2$$

The dependence of this distribution on the angle between the direction of orientation and the direction of emission, θ, is described by the Legendre polynomials $P_k(\cos\theta)$. The A_k depend on the spin of the initial state I_i, the final state I_f and the multipolarities involved in the gamma transition. For transitions with multipolarity 2^L all A_k with $k > 2L$ are zero. Explicit formulas for the A_k for pure dipole, quadrupole and octupole transitions and for mixed

dipole-quadrupole transitions can be obtained from expressions given in ref. 2. The disorientation due to possible preceding transitions is described by the G_k parameters. For a single transition between states with spins I_i and I_f in which an angular momentum j is carried off, G_k is given by the following expression:

$$G_k = \left(\frac{I_i}{I_f}\right)^k \left[\frac{(2I_f+1+k)!\,(2I_i-k)!}{(2I_i+1+k)!\,(2I_f-k)!}\right]^{\frac{1}{2}} (2I_i+1)\ W(I_f j\ kI_i; I_i I_f), \qquad 2.3$$

where the $W(I_f j\ kI_i; I_i I_f)$ are Racah coefficients. This formula is applicable for gamma transitions as well as for s-wave neutron capture. In the latter case $I_f = J = I_i \pm \frac{1}{2}$, where I_i is the spin of the target nucleus. For mixed gamma transitions or for neutron capture in which both spin states $J = I \pm \frac{1}{2}$ occur appropriately weighted averages must be used. For a cascade of gamma rays following neutron capture G_k can be written as:

$$G_k = G_k^n \prod_i G_k(\gamma_i), \qquad 2.4$$

where G_k^n and $G_k(\gamma_i)$ are related to the neutron capture and to the preceding gamma rays respectively. Explicit formulas of the $G_k(\gamma_i)$ for pure dipole, quadrupole and octupole transitions and for mixed dipole-quadrupole transitions are given in ref. 2 and the first two G_k^n with k even, which were needed for the interpretation of the experimental results, are as follows:

$$G_2^n = \frac{I^2(I+2)}{(I+1)(I+\frac{1}{2})^2} \quad \text{and} \quad G_4^n = \frac{I^4(I+3)}{(I+1)(I+\frac{1}{2})^4} \qquad \text{if } J = I+\tfrac{1}{2} \text{ and}$$

$$G_2^n = \frac{I(I-1)}{(I-\frac{1}{2})^2} \quad \text{and} \quad G_4^n = \frac{I^3(I-2)}{(I-\frac{1}{2})^4} \qquad \text{if } J = I-\tfrac{1}{2}. \qquad 2.5$$

A change in the orientation parameters may also take place during the finite lifetimes of the intermediate levels. However, the nuclear lifetimes in the experiments were supposed to be sufficiently short to neglect this influence.

For combinations of multipolarities which are not given in ref. 2 the A_k in formula 2.2 can be obtained from[3]:

$$A_k = \binom{2k}{k} I_i^k \left[\frac{(2k+1)\ (2I_i-1)\ \ (2I_i-k)!}{(2I_i+k+1)!}\right]^{\frac{1}{2}} F_k \,. \qquad 2.6$$

For a mixed transition with angular momenta L and L' the F_k parameters are:

$$F_k = \frac{1}{(1+\delta^2)} \left[F_k(LL\, I_f I_i) + 2\delta\, F_k(LL'\, I_f I_i) + \delta^2\, F_k(L'L'\, I_f I_i) \right] \qquad 2.7$$

The $F_k(L_1 L_2 I_1 I_2)$ are the well known parameters of Ferentz and Rosenzweig[4] which have been tabulated for many combinations of spins and multipolarities. The mixing parameter δ is the ratio of the reduced matrix elements of transitions with angular momenta L and L'. The mixing parameter used by Hartog e. a.[2] is both the opposite and the inverse of the parameter used by Ferentz and Rosenzweig[4]. The convention used in ref. 4 has been adopted in this thesis.

Experimentally the anisotropy, defined as $W(\theta)-1$, was measured by comparing the intensities of gamma rays from oriented and unoriented nuclei in the direction of orientation ($\theta=0^\circ$) and for some low energy transitions also in a direction perpendicular to the axis of orientation ($\theta=90^\circ$).

In general the gamma radiation from oriented nuclei is also polarized. Since nuclear alignment is invariant under space reflection it can be seen that there is no net circular polarization of gamma rays emitted by aligned nuclei. The linear polarization can be observed in a direction perpendicular to the axis of orientation. Using the convention of Tolhoek and Cox[1] the degree of linear polarization, P, is positive if the average value of the component of the electric vector of the polarized gamma rays in the plane through the direction of nuclear orientation and the direction of the gamma rays is larger than the component perpendicular to this plane and P is negative if it is smaller. The absolute value of P is that part of the gamma radiation which is fully polarized. General formulas for the degree of linear polarization of mixed dipole-quadrupole transitions can be found in ref. 2. The following relation can be derived from these formulas for pure dipole and pure quadrupole transitions:

$$P = \pi_i\, \pi_f\, \frac{W(0^\circ) - W(90^\circ)}{W(90^\circ)}\,, \qquad 2.8$$

where π_i and π_f are the parities of the initial and final levels. If the multipolarity of a gamma transition is 2^L the following relation between the parities and L holds:

$$\pi_i\, \pi_f = \pm\, (-1)^L, \qquad 2.9$$

where the + sign is valid for electric transitions and the - sign for magnetic transitions. The electric or magnetic character of a transition can often be determined if in addition to the anisotropy also the degree of linear polarization has been measured.

Experimentally the linear polarization was measured in a direction perpendicular to the axis of orientation ($\theta=90^{o}$) with the Compton polarimeter which is described in chapter III.

Among the high energy gamma transitions from the capturing state those having a high intensity are generally assumed to be dipole transitions. This assumption is partly based on theoretical considerations and partly on the fact that of the experimentally observed transitions the strongest have E1 character, transitions which have probably M1 character are much weaker while quadrupole transitions from the capturing state have hardly been observed. If the thermal neutron cross-section is due to a dominating resonance in the thermal region or if the spins of the contributing resonances are equal the interpretation of the anisotropy measurements of the high energy gamma transitions from the capturing state is rather simple. For pure dipole transitions the anisotropy in the 0^{o} direction is given by:

$$W(0^{o})-1 = +\left[\frac{3J^{2}}{2(J+1)(2J+3)}\right] f_2 G_2^n \quad \text{if} \quad I_f = J+1,$$

$$W(0^{o})-1 = -\left[\frac{3J}{2(J+1)}\right] f_2 G_2^n \quad \text{if} \quad I_f = J, \qquad 2.10$$

$$W(0^{o})-1 = +\left[\frac{3J}{2(2J-1)}\right] f_2 G_2^n \quad \text{if} \quad I_f = J-1.$$

A rough measurement of the anisotropy is often sufficient to determine the spin of the final state.

For the low energy transitions the interpretation of the experimental results is complicated by the fact that the product of disorientation parameters $\prod_i G_k(\gamma_i)$ cannot be calculated exactly since the level density, the spins of the intermediate levels and the multipolarities of the transitions are not known. If the number of cascades from the capturing state to an energy level, of which the disorientation parameter has to be determined, is very large a statistical theory can be used. In order to estimate the disorientation para-

meters a computer programme was developed in which the following assumptions were made: The energy level scheme is thought to be composed of discrete energy levels below a certain energy and a pseudo-continuum above it. The pseudo-continuum is divided into a finite number of energy intervals. Each interval is again divided into subgroups of different spins and parities. Transitions in the continuum are only possible between subgroups of different energies. Average transition probabilities were used which were assumed to be proportional to single particle estimates. The level density in the continuum as a function of the energy E and the spin J is given by[5]:

$$\rho(E,J) = \frac{2J+1}{2\sqrt{2}\pi\sigma^3} \cdot \exp\left\{-\frac{(J+\frac{1}{2})^2}{2\sigma^2}\right\} \cdot \rho_0(E), \qquad 2.11$$

where

$$\rho_0(E) = \frac{\sqrt{\pi}}{12a^{\frac{1}{4}}U^{\frac{5}{4}}} \cdot \exp(2\sqrt{aU}) \qquad \text{and} \qquad U = E - \Delta.$$

U is the effective excitation energy, σ is the spin cut-off parameter, Δ is the pairing energy and a denotes a parameter which is related to the single-proton and single-neutron level densities. Several authors attempted to derive a, σ and Δ from observed level densities, isomeric cross-section measurements[6,7] etc. Starting with assumed values of σ and Δ the parameter a was adjusted in such a way that expression 2.11 reproduced the experimental neutron resonance density near the binding energy.

By means of a computer programme the decay of the nuclei was simulated with a Monte-Carlo procedure. In addition to the disorientation parameters the programme could calculate the multiplicity, which is the average number of transitions from the capturing state to the ground state, the occupation numbers of levels with different spins in the continuum and the shape of the spectrum in the continuum. The dipole-quadrupole mixture and the parameters σ and Δ have been varied to see their influence on the multiplicity and the disorientation parameters.

In general the variations were rather small. Even if the transition probabilities of dipole and quadrupole transitions (for one MeV radiation) are taken to be equal, the influence on the disorientation parameters is negligible. The parameter σ which, according to different authors[5,6], is of the order of 3-5, did not vary the disorientation parameters by more than 6 %, while the influence

due to a reasonable change of Δ is still less. The disorientation parameters of ^{144}Nd and ^{150}Sm can be found in table 4.VI and 5.VIII respectively. In addition to the parameters calculated with the computer programme also the results of a much simpler calculation are given in which it was assumed that there are only dipole transitions and in which the number of transitions in a cascade, ν, was kept fixed. The results of both calculations are about the same if the difference between the spin of the capturing state and the spin of the final level is not large.

REFERENCES

1. Tolhoek, H.A. and Cox, J.A.M., Physica 19 (1953) 101.
2. Hartog, Chr.D., Tolhoek, H.A. and De Groot, S.R., Physica 20 (1955) 1310.
3. De Groot, S.R., Tolhoek, H.A. and Huiskamp, W.J., Alpha- Beta- and Gamma-Ray Spectroscopy, Volume 2, Chapter XIXB, edited by K.Siegbahn. (North Holland Publ. Comp. Amsterdam, 1965).
4. Ferentz, M. and Rosenzweig, N., A.N.L. Report 5324.
5. Ericson, T., Adv. Phys. 9 (1960) 425.
6. Newton, T.D., Can. J. Phys. 34 (1956) 804.
7. Gilbert, A. and Cameron, A.G.W., Can. J. Phys. 43 (1965) 1446.

CHAPTER III

EXPERIMENTAL ARRANGEMENT

The experiments were performed at the high flux reactor in Petten. This reactor has ten radial beam tubes which can be used for neutron diffraction and nuclear physics experiments. The flux in these tubes near the reactor core is about 3×10^{13} neutrons/cm^2.s at a reactor power of 30 MW. These primary beams are not directly suitable for experiments with thermal neutrons since there is a large contamination of fast neutrons and gamma rays. Among several possible ways for removing this contamination the method of diffraction at a single crystal, of total reflection at mirrors and of transmission through a neutron filter are most often used. Two neutron beams were used in the experiments described in the next chapters.

A horizontal cross-section of the diffraction set-up used for the experiments with oriented nuclei is given in fig. 3.1. The primary circular neutron beam from the reactor is collimated to a diameter of 6 cm and then diffracted by a single crystal of copper. A rotary shutter which can be opera-

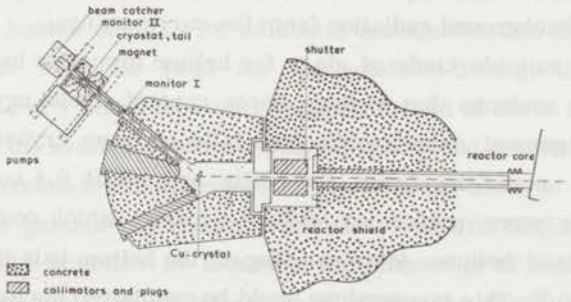

Fig. 3.1. Horizontal cross-section of the neutron beam and the nuclear orientation set-up.

ted with an electric motor is present between the collimator and the diffraction set-up. There are two positions available for the monochromator. In one position the angle between the primary beam and the diffracted beam is 25^{o}, while in the other position the angle is either variable between 4^{o} and 16^{o} or 37^{o}. Only the latter arrangement with the fixed angle was used. The monochromator is a single crystal of copper 5 cm in diameter and 5 mm thick used in transmission. The reflected beam is collimated again. The diameter near the sample is 2.5 cm. Reflections at the (111) planes and (022) planes have been used. If the primary neutron beam was reflected at the (111) planes, the intensity of the diffracted monochromatic beam, with a neutron energy of 0.047 eV, was 1.6×10^{6} neutrons/cm^{2}.s. The contribution of higher order reflections may have been about 7 %. This intensity gives reasonable counting rates for the gamma-ray detectors while the heat input in the samples due to radiation is sufficiently low for performing experiments with samples at about 0.01 K. After reflection at the (022) planes the neutron energy is 0.125 eV. In this case the intensity was 0.4×10^{6} neutrons/cm^{2}.s. Near the sample the beam is shielded with LiF enriched in ^{6}Li in order to reduce the background due to neutron capture in the surrounding material.

The spectra of isotopically enriched samples were obtained using another neutron beam with a higher intensity. For this beam a filter consisting of quartz and bismuth single crystals cooled to liquid nitrogen temperature was used in order to remove fast neutrons and gamma rays. At the position of the sample the intensity was 10^{7} neutrons/cm^{2}.s. Near the sample the beam was again shielded with LiF enriched in ^{6}Li and also with lead in order to reduce the background radiation from the surroundings.

Since suitable kinds of glass for helium cryostats have a large cross-section for neutrons due to their boron content, metal cryostats were used for the alignment experiments. The tails of these cryostats were made of aluminium; near the beam the walls are about 0.4 mm thick. The first experiments were performed with a cryostat which could hold about five liters of liquid helium. After pumping off the helium bath the final temperature was 1.0 K. This temperature could be maintained during one to two days. Since long term measurements became more and more frequent a bigger cryostat was constructed with which measurements during a period of four to five days are possible without refilling with helium.
The two helium baths of this cryostat are shown in fig. 3.2. The outside

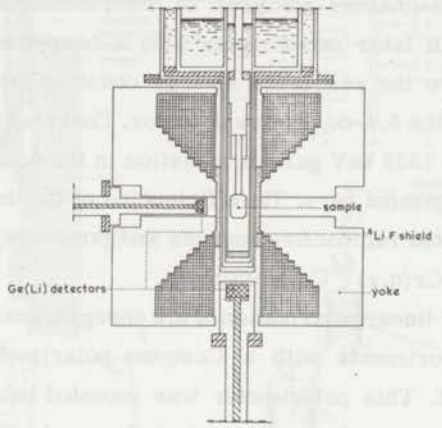

Fig. 3.2. A sketch of a part of the experimental set-up showing the magnet for adiabetic demagnetization, the cryostat and the Ge(Li) detectors.

helium bath can hold ten liters of liquid helium and the other bath about five liters. During the experiments the helium in the outside bath was boiling under atmospheric pressure (4.2 K). The evaporation rate was 60 cc per hour. The other helium bath was pumped off to 1.0 K and under running conditions the evaporation rate was about 25-30 cc per hour. A sample which is mounted in a holder suitable for adiabatic demagnetization is also shown in fig. 3.2. The magnetic field for the adiabatic demagnetizations was obtained by the aid of a small iron-core magnet. A field of about 13 kOe could be obtained with the available power supply. The size and construction of the magnet made it possible to mount the detectors sufficiently close to the sample.

The capture gamma-ray spectra were measured with Ge(Li) detectors. In principe it was possible to measure the anisotropy of capture gamma rays from aligned nuclei in the direction of orientation ($\theta=0^{\circ}$) and perpendicular to this direction ($\theta=90^{\circ}$). The two detectors, an R.C.A. detector with an active volume of 2 cc and a 6.4-cc Philips detector, are indicated in fig. 3.2. In some of the experiments another R.C.A. detector having an active volume of 5 cc was used. The electronic equipment for each de-

tector consisted of a combination of Ortec or Nuclear Enterprises amplifiers and a multi-channel pulseheight analyser. The available analysers were a 400- and a 4096-channel analyser of Intertechnique and a Laben 4096-channel analyser. In later experiments also a base-line restorer was used in order to improve the resolution at high counting rates. The best results were obtained with the 6.4-cc Philips detector. The resolution of this detector was 3.5 keV for the 1333 keV gamma radiation in the decay of ^{60}Co and about 8 keV for 7.5 MeV gamma rays. The efficiencies of the detectors were determined with calibrated radioactive sources and gamma rays from the H(n,γ)D, ^{12}C(n,γ)^{13}C and ^{53}Cr(n,γ)^{54}Cr reactions.

The degree of linear polarization of low energy transitions was measured in one of the experiments with a Compton polarimeter of which a sketch is given in fig. 3.3. This polarimeter was mounted below the magnet and it viewed the gamma rays from the oriented sample through the tail of the cryostat. As a scatterer a NaI(Tl) crystal, 50 mm high and 44 mm in diameter, was used. It was located at a distance of 23 cm from the target, just outside the magnet. The two side detectors were also cylindrical NaI(Tl) crystals, 75 mm high and 75 mm in diameter. The distances between the centres of these side crystals and the centre of the scatterer was about 8 cm. These distances were chosen as short as possible in order to get an acceptable counting rate. Compton scattering of a beam of linearly polarized gamma rays occurs preferentially in a plane perpendicular to the electric vector of the incident radiation. Let $N_{\parallel}$ be the number of gamma rays scattered by S and detected by $D_{\parallel}$ and $N_{\perp}$ the number of gamma rays scattered by S and detected by $D_{\perp}$. Then the following equation is valid (see fig. 3.3 b):

$$\frac{N_{\perp}}{N_{\parallel}} = \frac{1+\overline{Q}\cdot P}{1-\overline{Q}\cdot P} \quad , \qquad 3.1$$

were P is the degree of linear polarization of the radiation and $\overline{Q}$ is the quality factor of the polarimeter [1,2]. $\overline{Q}$ depends on the scattering angles as well as on the energy of the radiation. The gamma rays can scatter into the side crystals over a rather large solid angle. Therefore an average value of Q must be used. For gamma rays of 750 keV an optimum value of Q is reached for a scattering angle $\chi = 72^{\circ}$. The side crystals were positioned to achieve roughly this angle. The pulses from the detectors $D_{\parallel}$ and $D_{\perp}$ were added separately to the pulses from S as has been indi-

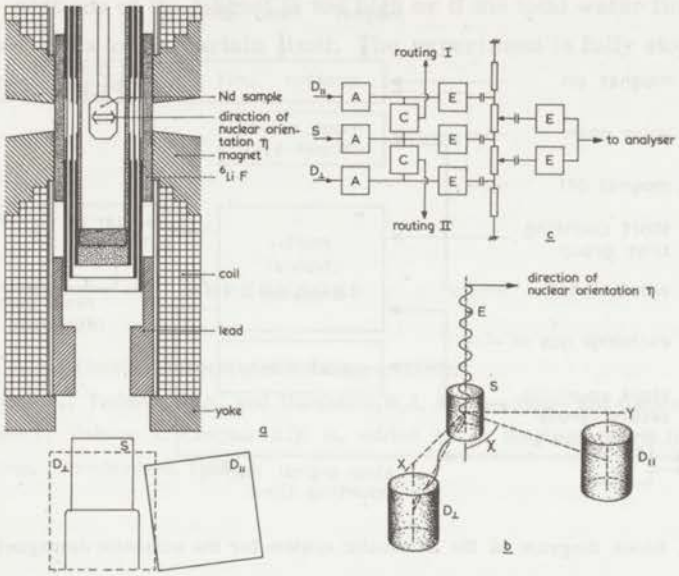

Fig. 3.3.a. A sketch of the cryostat tail, the magnet for adiabatic demagnetization and the Compton polarimeter used for measuring the linear polarization of gamma rays emitted perpendicular to the axis of nuclear orientation.

b. Schematic drawing of the Compton polarimeter.

c. Block-diagram of the electronics.

A is amplifier, C is coincidence unit, and E is emitter follower.

cated in fig. 3.3c. Each sum pulse was routed into a 100-channel subgroup of a 400-channel Intertechnique analyser. Only gamma rays coincident in S and one of the side crystals were accumulated in the appropriate subgroups. The resolving time of the coincidence units was about 40 ns. The average value of Q is expected to be about 0.3 to 0.5 for energies between 0.5 and 1 MeV [1]. It can be obtained by numerical integration of the Klein-Nishina formula for Compton scattering. $\overline{Q}$ can also be derived in an experimental way by measuring the linear polarization of known transitions. The latter approach was possible in the experiment with neodymium nuclei which is described in chapter IV.

At first the adiabatic demagnetizations were performed manually. However, since the experiments had to be continued for weeks in order

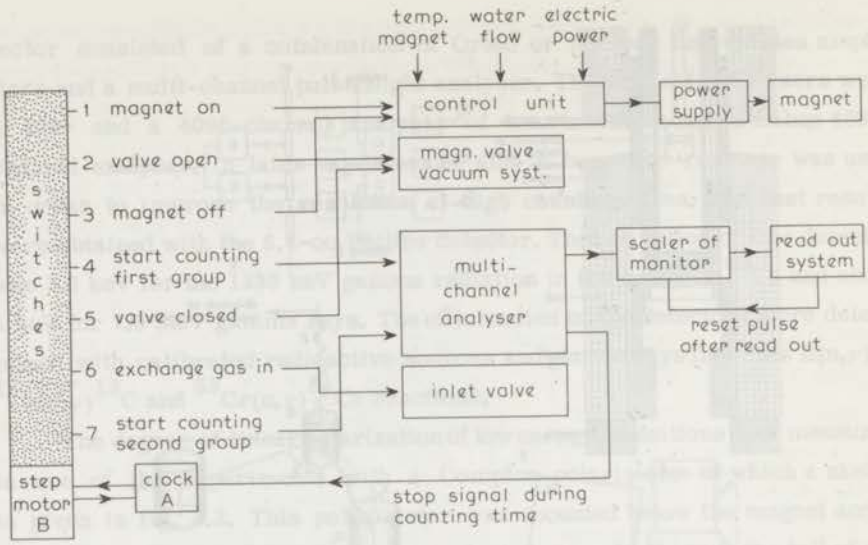

Fig. 3.4. Block diagram of the automatic system for the adiabatic demagnetizations.

to get sufficient statistical accuracy the equipment was fully automated. Fig. 3.4 gives a block diagram of the whole system. The main component of this system is a multi-circuit timer consisting of a clock A, a step motor B and a roll which can operate twenty switches. A cycle was performed in twenty steps and the time between two successive steps was determined by the clock A. The operations which were performed in succession in each cycle are indicated by the numbers 1-7 in fig. 3.4 and can be programmed at will. In the first step of the cycle the magnet is switched on. The heat of magnetization is conducted to the 1.0 K helium bath via the helium contact gas. Next the sample is thermally isolated by pumping away this contact gas. The final pressure is of the order of 10^{-6} Torr. In the next stage the magnetic field is diminished to zero and the temperature of the sample will drop to about 0.01 K. Under this condition the nuclei are oriented and the analyser is started for a certain counting period. After this counting time the sample is warmed up by letting in some contact gas. In the last step the analyser is started again for the same length of time as after the adiabatic demagnetization. The spectra which were measured at 0.01 K and about 1.0 K were accumulated in two different groups of the analyser.

During the measuring time the clock A was stopped. The intensity of the neutron beam was monitored with a BF_3 counter. After each counting period of the analyser the scaler of the monitor was read out and reset. The control unit for the magnet turns off the power supply if the temperature of one

of the 26 sections of the magnet is too high or if the total water flow through the magnet is below a certain limit. The experiment is fully stopped after an electric power failure.

REFERENCES

1. Diddens, A.N., Thesis, University of Groningen (1957).
2. De Groot, S.R., Tolhoek, H.A. and Huiskamp,W.J. Alpha-, Beta- and Gamma-Ray Spectroscopy, Volume 2, Chapter XIX B, edited by K. Siegbahn (North Holland Publ. Comp. , Amsterdam, 1965).

CHAPTER IV

NEUTRON-CAPTURE GAMMA-RAY SPECTRA FROM ^{143}Nd and ^{145}Nd INCLUDING ANISOTROPY AND LINEAR POLARIZATION MEASUREMENTS OF NEUTRON-CAPTURE GAMMA RAYS FROM ALIGNED ^{143}Nd NUCLEI

1. Introduction

Natural neodymium consists of several stable isotopes. Only ^{143}Nd and ^{145}Nd have considerable cross-sections for thermal neutrons. No data of a systematic study of capture gamma rays from the stable neodymium isotopes were available when the nuclear orientation experiments with a sample containing natural neodymium were started. In order to find out which of the gamma rays are due to capture in ^{143}Nd and which to capture in ^{145}Nd, capture gamma-ray spectra of samples enriched in these isotopes were studied at the high flux reactor in Petten. Recently the capture gamma-ray spectrum of natural neodymium was studied by Groshev e.a.[1] with a magnetic Compton spectrometer and a Ge(Li) detector. In addition he also studied the spectra of samples enriched in the stable neodymium isotopes with the exception of ^{148}Nd and ^{150}Nd of which practically no influence on the spectrum of natural neodymium is expected since their capture cross-sections and abundances are very low.

The anisotropy in the directional distribution of capture gamma rays from aligned ^{143}Nd nuclei was measured in the direction of nuclear orientation. In this way several spin values of energy levels were determined. For some low energy transitions the degree of linear polarization was measured which gave extra information about the character of two low energy transitions. No anisotropies of gamma rays following neutron capture in ^{145}Nd were measured since the intensity of the observed transitions was too low.

The available data of the nuclei ^{144}Nd and ^{146}Nd have recently been compiled in the Nuclear Data Sheets [2]. Additional information can be found in the following recent publications. The decays of ^{144}Pm and ^{144}Pr

have been reinvestigated using gamma-gamma coincidence and angular correlation techniques. The β-decay of ^{144}Pm was studied by Eissa e.a.[3], by Raman[4], by Santhanam e.a.[5] and by Barette e.a.[6], while the β-decay of ^{144}Pr was reinvestigated by Hübel e.a.[7] and by Raman[8]. The conversion coefficients of two gamma transitions in the decay of ^{144}Pm were compared by Avotina e.a.[9]. Additional information on the energy level scheme of ^{146}Nd was obtained by Tailor and Kukoč[10]. They studied the gamma-ray spectrum and some gamma-gamma coincidences in the β-decay of ^{146}Pm.

2. Alignment of neodymium nuclei.

A suitable material for nuclear orientation of neodymium isotopes is $Nd(C_2H_5SO_4)_3.9H_2O$. The thermal and magnetic properties of this substance have been investigated by Meyer [11] and more recently by Blok e.a. [12]. Starting from the conditions in our experiment (viz. an initial temperature of 1.0 K and a magnetic field of 12.9 kOe along the c-axis of a single crystal of neodymium ethylsulphate) a final temperature of 0.014 K will be reached after adiabatic demagnezation. The magnetic properties of neodymium ions in a single crystal of lanthanum (neodymium) ethylsulphate can be described by the effective-spin Hamiltonian [13]:

$$\mathcal{H} = g_{\parallel}\mu_B H_z S_z + g_{\perp}\mu_B (H_x S_x + H_y S_y) + A S_z I_z + B(S_x I_x + S_y I_y) + P\{I_z^2 - \tfrac{1}{3}I(I+1)\}. \qquad 4.1$$

For ^{143}Nd the following constants are known: the nuclear spin $I = 7/2$; the effective electron spin $S = 1/2$; the splitting factors are $g_{\parallel} = 3.535$ and $g_{\perp} = 2.072$ and the hyperfine splitting constants are $A/k = 0.0543$ K, $B/k = 0.0285$ K and $P/k = 8.10^{-5}$ K [13].

The first two alignment parameters have been calculated using this Hamiltonian assuming that the constants given above are also valid for neodymium ethylsulphate. The results are $f_2 = 0.348$ and $f_4 = 0.033$ at a temperature of 0.014 K.

The sample used in the alignment experiments consisted of two single crystals of neodymium ethylsulphate with a total weight of 5.5 g. The crystals were mounted in such a way that the c-axes which are also the axes of nuclear alignment, were perpendicular to the direction of the neutron beam and to the axis of the cryostat tail. After demagnetization the sample could be kept at a temperature of 0.014 K for a period of one hour.

3. Neutron capture by neodymium

Natural neodymium has a total cross-section of 54 barns [14] at the neutron energy of 0.047 eV used in the nuclear orientation experiments. The capture cross-section is 37 barns and 75 % of this capture is due to ^{143}Nd. The large cross-section of ^{143}Nd is generally attributed to a bound level [15] (negative resonance); the next two resonances occur at 55.8 and 128 eV and their contributions to the capture cross-section of ^{143}Nd is less than 0.8 %. The spins of the resonances of ^{143}Nd have been derived from neutron cross-section measurements and also from studies of the gamma and alpha spectra following neutron capture in these resonances [15,16]. The spins of the negative resonance and of the resonance at 128 eV are 3 while the spin of the weak resonance at 55.8 eV is uncertain but spin 4 is more likely than spin 3. The contribution of ^{145}Nd to the capture cross-section of natural neodymium is 9.4 %. The lowest three resonances have been observed at 4.36, 43.1 and 86.5 eV. The spins of these three resonances are 3 [15,16]. They have been determined with the same methods as in the case of ^{143}Nd. The capture cross-sections of the other stable isotopes at thermal energy are given in table 4.I.

Table 4.I.

Thermal neutron-capture cross-sections and neutron-binding energies of the stable neodymium isotopes.

isotope	cross-section in barns [14,15]	neutron binding energy [20] in keV
^{142}Nd	18 ± 2	9809 ± 14
^{143}Nd	335 ± 10	6100 ± 7
^{144}Nd	5.0 ± 0.6	7830 ± 6
^{145}Nd	52 ± 2	5744 ± 6
^{146}Nd	10 ± 1	7561 ± 6
^{148}Nd	2.9 ± 0.5	7331 ± 12
^{150}Nd	1.8 ± 0.3	7332 ± 11

4. Experimental results

a. Capture gamma-ray spectra of natural neodymium and of isotopically enriched neodymium samples.

The isotopic and spectrographic analyses of the samples enriched in

^{143}Nd and ^{145}Nd used in the experiment are given in table 4.II, together with the isotopic composition of natural neodymium. All the samples were in the form of Nd_2O_3. The enriched samples were obtained on loan for a few months from the electromagnetic separation group of the U.K.A.E.R.E. at Harwell.

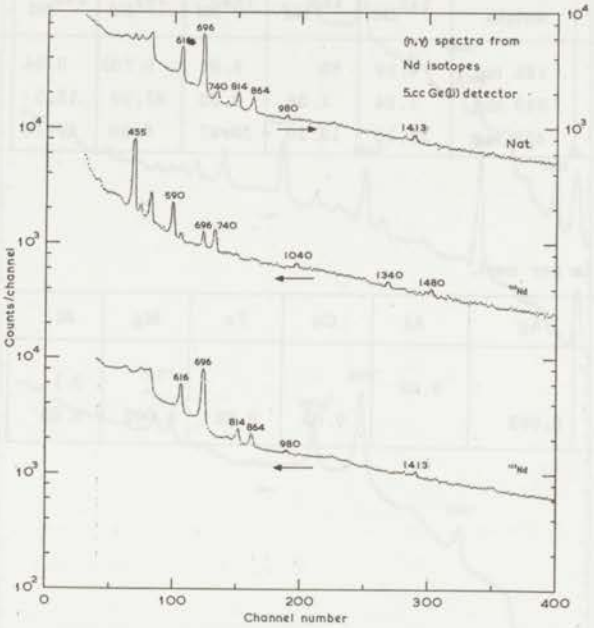

Fig. 4.1. Low energy parts of the neutron-capture gamma-ray spectra from enriched neodymium samples and a sample of natural neodymium measured with the 5-cc Ge(Li) detector. The energies are given in KeV.

Relevant parts of the spectra of the enriched samples and of natural neodymium are given in fig. 4.1 to 4.3. Single escape peaks are indicated by a single prime, double escape peaks have a double prime and photopeaks are not indicated. The spectra of fig. 4.1 and 4.2 were obtained with the 5-cc R.C.A. detector and a 400-channel analyser. The high energy part of the spectrum of natural neodymium which was measured with the 6.4-cc Philips detector and a 4096-channel analyser is given in fig. 4.3. Not all channels are plotted in this figure: in regions where there are no peaks visible each second point is given only. Each part of this spectrum covers 512 channels. The spectrum is very complicated in the energy region between 1.5 and 4.5 MeV and impossible to unravel in a useful way. Therefore this part of the spectrum has been omitted.

Low energy parts of the spectra of natural neodymium and of the enriched samples are given in fig. 4.1. A comparison of the spectra shows

Table 4.II.

Percentage composition of the enriched neodymium samples.

sample	weight	^{142}Nd	^{143}Nd	^{144}Nd	^{145}Nd	^{146}Nd	^{148}Nd	^{150}Nd
^{143}Nd	128 mg	4.09	85	8.91	0.702	0.54	0.66	0.048
^{145}Nd	340 mg	1.54	1.38	6.92	67.90	12.5	0.59	0.16
natural	450 mg	27.13	12.20	23.87	8.30	17.18	5.72	5.60

Impurities in per cent.

sample	Ag	Al	Cu	Fe	Mg	Si	Pb
^{143}Nd		0.02				0.1	0.06
^{145}Nd	0.003		0.03	0.02	0.002	0.03	

which of the peaks are due to capture in ^{143}Nd and which to capture in ^{145}Nd. It can be seen that the peak at 740 keV is increased in the second spectrum of fig. 4.1, where it is mainly related to capture in ^{145}Nd. However, the corresponding peak in the spectrum of natural neodymium is to a large extent due to the 740 keV ground state transition in ^{143}Nd[1)].

High energy parts of the spectra of natural neodymium and of the enriched neodymium samples are given in fig. 4.2. The spectrum of natural neodymium was measured again in a later stage of the experiments. The high energy part of this spectrum is given in fig. 4.3. The peaks in this figure are much better resolved than in the corresponding spectrum of fig. 4.2. It can be concluded from these spectra and from the results given in ref. 1 to which isotopes the transitions belong.

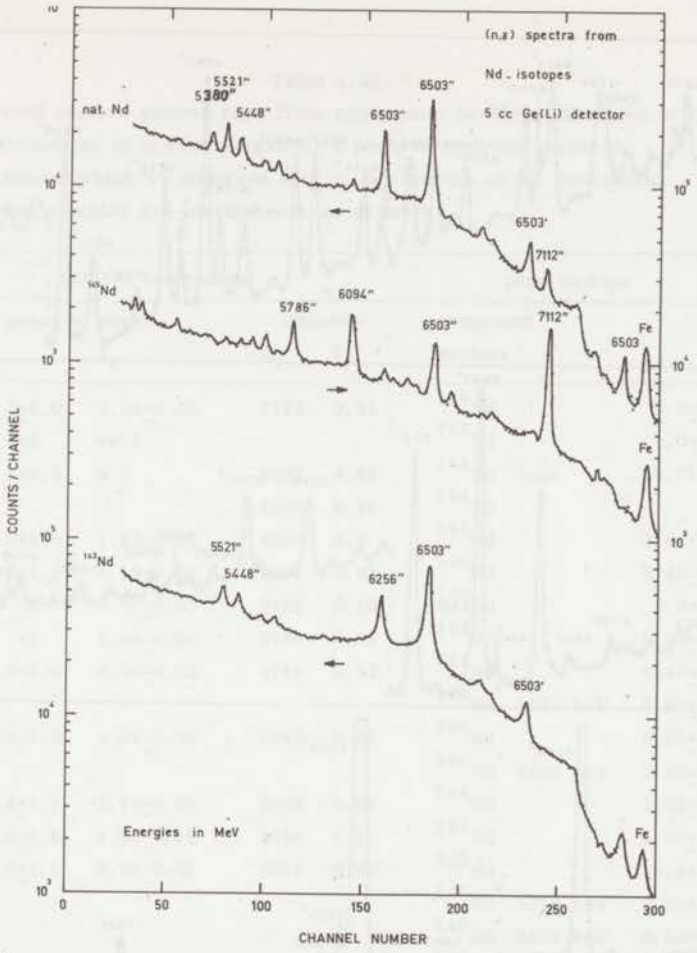

Fig. 4.2. High energy parts of the neutron-capture gamma-ray spectra from enriched neodymium samples and a sample of natural neodymium measured with the 5-cc Ge(Li) detector. The energies are given in keV.

The recoil corrected energies and the intensities of the observed high energy transitions in natural neodymium are given in table 4.III together with the results obtained by Groshev[1] with a Compton spectrometer. The intensity of the 6502.8 keV transition of ^{144}Nd was assumed to be 4.3 gamma's per 100 neutrons captured which is an averaged value of the results obtained by Groshev[1]. The compound nuclei to which the transitions belong are given in the fifth column of table 4.III. In addition the intensities obtained for the pure isotopes are given. They were calculated using the capture cross-sections and abundances of the isotopes. The energies of the low energy transitions are also given in table 4.III. The corresponding intensities were calculated relatively to the intensity of the 696 keV transition given in ref. 1 and 2.

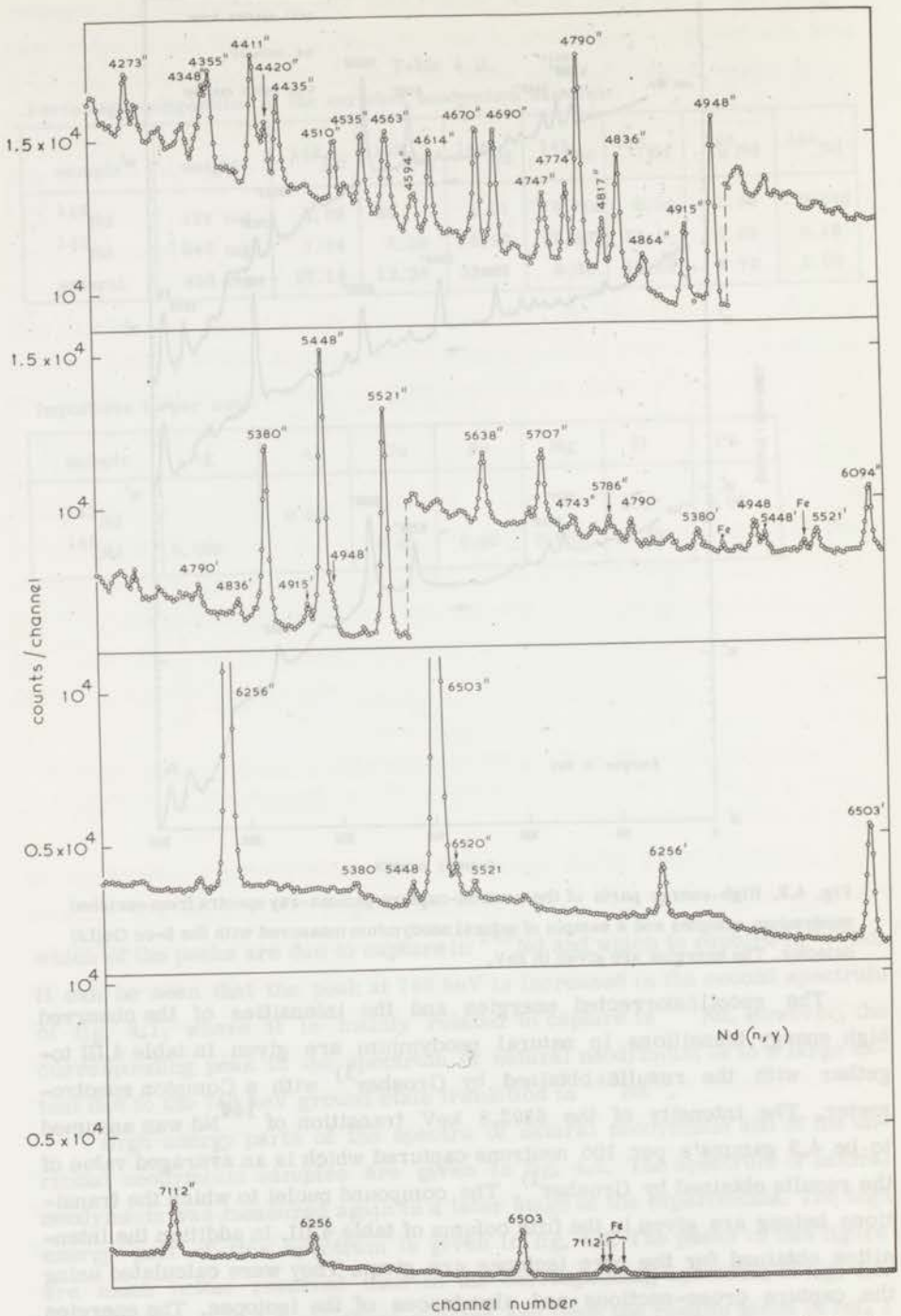

Fig. 4.3. High energy part of the neutron-capture gamma-ray spectrum of natural neodymium measured with the 6.4-cc Ge(Li) detector. The energies are given in keV.

Table 4. III.

Observed capture gamma rays from neodymium isotopes. Energies in keV and intensities in number of gamma's per 100 neutrons captured. Transitions which we observed only in the spectra of the isotopically enriched samples are marked with an arterisk.

natural neodymium				pure isotope	
present work		Groshev		compound	
E_γ	I_γ	E_γ	I_γ	nucleus	I_γ
7112.0±1.0	0.24±0.03	7113	0.35	^{146}Nd	3.0±0.4
6520 ±2	~0.1			^{146}Nd	1.0±0.3
6502.8±1.0	4.3	6503	4.03	^{144}Nd	5.71
		6308	0.04	^{144}Nd	
6256.2±1.0	1.83±0.02	6260	2.3	^{144}Nd	2.44±0.03
6094.0±1.0	0.19±0.03	6097	0.23	^{146}Nd	2.40±0.04
5786 ±2	0.07±0.03	5792	0.13	^{146}Nd	0.9±0.4
5743 ±2	0.05±0.02	5748	0.05	(^{144}Nd)	0.07±0.03
5707.0±1.2	0.30±0.03	5712	0.33	^{144}Nd	0.40±0.04
				^{146}Nd* 5650 keV	0.40±0.08
5637.8±1.2	0.26±0.03	5645	0.31	^{144}Nd	0.35±0.04
				^{146}Nd* 5600 keV	0.08±0.02
5521.4±1.0	0.78±0.08	5528	0.84	^{144}Nd	1.04±0.11
5448.1±1.0	1.20±0.12	5454	1.15	^{144}Nd	1.60±0.17
5379.9±1.0	0.65±0.07	5389	0.80	^{143}Nd	10.4±0.8
				^{146}Nd* 5210 keV	0.23±0.10
				^{146}Nd* 5050 keV	0.30±0.15
				^{146}Nd* 5020 keV	0.40±0.15
4948.4±1.5	0.62±0.06	4953	0.97	^{144}Nd	0.83±0.09
4915.3±1.5	0.27±0.04	4921	0.27	^{144}Nd	0.36±0.06
4864 ±2	0.10±0.04	4869	0.13	^{144}Nd	0.13±0.05
4836.0±1.5	0.43±0.05	4845	0.54	^{144}Nd+^{145}Nd	
4816.9±1.7	0.15±0.03	4827	0.26	^{143}Nd	2.4 ±0.8
4790.2±1.7	0.71±0.07	4796	0.70	^{144}Nd	0.95±0.10
4774.0±1.7	0.25±0.04	4780	0.30	^{144}Nd	0.33±0.06
4746.5±1.8	0.29±0.05	4756	0.43	^{144}Nd	0.39±0.07
4690.1±1.8	0.39±0.05	4699	0.48	^{144}Nd +^{147}Nd	-
4670.2±1.8	0.42±0.05	4678	0.51	^{144}Nd +^{147}Nd	-
4614.4±1.8	0.24±0.03	4624	0.35	^{144}Nd	0.32±0.04
4594 ±2	0.13±0.04	4605	0.21	^{144}Nd	0.17±0.06

Table 4.III (continued)

E_γ	I_γ	E_γ	I_γ	compound nucleus	I_γ
4562.7±1.8	0.41±0.09	4570	0.49	^{144}Nd	0.55±0.13
4534.5±1.8	0.27±0.05	4542	0.50	^{144}Nd	0.36±0.07
4510 ±2	0.19±0.04	4509	0.42	^{144}Nd	0.25±0.06
4435 ±2	0.17±0.05	4440	0.46	^{144}Nd	0.23±0.07
4420 ±2	0.08±0.03			^{146}Nd+^{144}Nd	-
4411 ±2	0.26±0.06	4410	0.74	^{144}Nd	0.35±0.09
				^{146}Nd* 1480 keV	1.8 ±0.4
1413	3.1 ±0.5			^{144}Nd	3.1 ±0.5
				^{146}Nd*1340 keV	1.6 ±0.4
				^{146}Nd*1040 keV	1.7 ±0.4
980	1.5 ±0.2	978	4.6	^{144}Nd	2.0 ±0.4
864	8.0 ±0.08	864	12.5	^{144}Nd	1.1 ±0.1
814	8.0 ±0.08	811	12.0	^{144}Nd	1.1 ±0.1
740	5.9 ±0.1	736	8.2	^{143}Nd+^{146}Nd	-
696	60	696	66.2	^{144}Nd	80
616	24 ±3	616	28.8	^{144}Nd	32 ±5
				^{146}Nd* 590 keV	14 ±3
455	3.7 ±0.7			^{146}Nd	47 ±11

b. Anisotropy measurements.

The total background at each peak was determined by fitting a straight line through suitably chosen intervals of points on the left and right of the peak. The areas, S, of the peaks were obtained after subtraction of the background. The experimental anisotropy, which is defined as [S(0.01 K) - S(1.0 K)]/S(1.0 K), was calculated for each peak separately. Fig. 4.4 shows as an example a part of the high energy spectrum measured in the direction

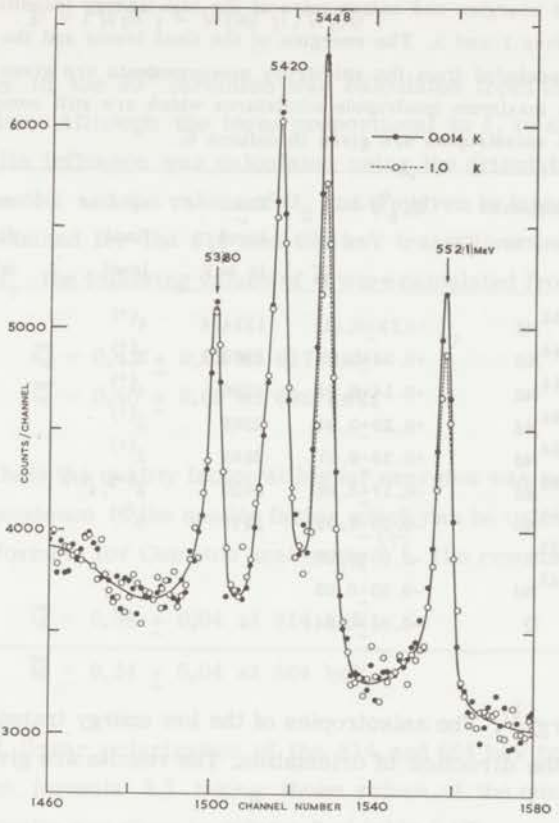

Fig. 4.4. Quartet of lines at approximately 5.5 MeV measured with the 2-cc Ge(Li) detector along the direction of nuclear orientation with the sample at 1 K and 0.014 K.

of nuclear orientation at 1.0 K and 0.01 K. The spectrum at 0.01 K was corrected for a 7 % anisotropy in the background which is related to Compton scattered gamma rays of transitions of higher energies. The peak at 5380 keV is due to capture in the even-even isotope ^{142}Nd and the 5420 keV peak is due to the sulphur in neodymium ethylsulphate. Consequently no anisotropy is expected for these transitions. Fig. 4.4 shows that this is indeed the case. Neither the capture gamma rays from hydrogen show an anisotropy. The transitions at 5448 and 5521 keV in fig. 4.4 are both due to ^{144}Nd and show anisotropies of +28 % and +14 %, respectively. The anisotropies of other high energy transitions can be found in table 4.IV. The anisotropy of the 4690 keV transition was corrected for the influence of a transition in ^{147}Nd which has

Table 4.IV.

The measured energies and anisotropies of the high energy transitions are given in columns 1 and 3. The energies of the final levels and the spins which were concluded from the anisotropy measurements are given in column 4 and 5. The maximum quadrupole admixtures which are still comptable with the measured anisotropies are given in column 6.

E_γ in KeV	compound nucleus	$W(0^o)-1$	final level in keV	spin of final level	maximum quadrupole admixture in %
6502.8	^{144}Nd	$+0.12\pm0.01$	1314.4	$4^{(+)}$	0.02
6256.2	^{144}Nd	$+0.34\pm0.03$	1560.1	$2^{(+)}$	0.15
5521.4	^{144}Nd	$+0.14\pm0.04$	2296	$4^{(+)}$	0.18
5448.1	^{144}Nd	$+0.28\pm0.04$	2369	$2^{(+)}$	0.15
4948.1	^{144}Nd	$+0.33\pm0.07$	2869	$2^{(+)}$	0.33
4790.2	^{144}Nd	$+0.17\pm0.08$	3027	$2^{(+)}, 4^{(+)}$	1.6
4690.1	^{144}Nd	-0.25 ± 0.09	3127	$3^{(+)}$	7.8
5420	^{33}S	-0.05 ± 0.05			
5379.9	^{143}Nd	-0.03 ± 0.05			
2224	D	-0.01 ± 0.04			

the same energy[1]. The anisotropies of the low energy transitions were also measured in the direction of orientation. The results are given in table 4.V.

c. Linear polarization measurements.

The measured values of $N_\perp/N_\parallel$ and $W(0^o)-1$ of the low energy transitions are given in table 4.V. The transitions at 616 and 696 keV were used

Table 4.V.

Linear polarization and anisotropy of some low energy transitions in ^{144}Nd.

E_γ in keV	$N_\perp/N_\parallel$	$W(0^o) - 1$
617	0.75 ± 0.03	-0.267 ± 0.010
696	0.80 ± 0.02	-0.215 ± 0.010
814	0.78 ± 0.03	$+0.158 \pm 0.025$
864	0.85 ± 0.04	$+0.077 \pm 0.013$

to determine the quality factor of the polarimeter. Both are pure E2 transitions for which the following relation holds: (see formulas 2.8 and 2.9)

$$P = [W(0^{\circ}) - W(90^{\circ})]/W(90^{\circ})$$

The anisotropy in the 90° direction was calculated from the anisotropy in the 0° direction. Although the term proportional to f_4 is small, it can not be neglected. Its influence was calculated using the orientation parameters of the ^{143}Nd nuclei and the values of G_2 and G_4 given in table 4.VI. With the values of P obtained for the 616 and 696 keV transitions and the measured values of $N_{\perp}/N_{\parallel}$ the following values of $\bar{Q}$ were calculated from formula 3.1:

$$\bar{Q} = 0.41 \pm 0.05 \text{ at } 617 \text{ keV}$$

and

$$\bar{Q} = 0.40 \pm 0.05 \text{ at } 696 \text{ keV}.$$

From these values the quality factor at higher energies was estimated, using the energy dependence of the quality factor which can be calculated from the Klein-Nishina formula for Compton scattering [17]. The results are:

$$\bar{Q} = 0.36 \pm 0.04 \text{ at } 814 \text{ keV}$$

and

$$\bar{Q} = 0.34 \pm 0.04 \text{ at } 864 \text{ keV}.$$

The degree of linear polarization of the 814 and 864 keV transitions were calculated from formula 3.1 taking these values of the quality factor into account. The results are given in column 3 of table 4.VII.

Table 4.VII.

The energy E_γ, anisotropy $W(0^{\circ})-1$ and degree of linear polarization P of the 813.5 and 863.6 keV transitions in ^{144}Nd are given in column 1, 2 and 3. The multipole mixtures for the possible transitions given in column 4 which are compatible with the measured anisotropies and degrees of linear polarization can be found in column 6.

E_γ in keV	$W(0^{\circ}) - 1$	P	transition	possible multipole mixtures	conclusions
814	$+0.158 \pm 0.025$		$3^- \rightarrow 2^+$	99-100% E1 0-1% M2 2-7% E1 93-98%M2	99-100% E1 0 - 1% M2
		-0.35 ± 0.06		44-100% E1 0-56%M2	
864	$+0.077 \pm 0.013$		$2^+ \rightarrow 2^+$	70-83% M1 17-30%E2 0 - 3% M1 97-100%E2	70-83% M1 17-30% E2
		-0.23 ± 0.07		67-94% M1 6-33% E2	

5. Analysis of results

a. Anisotropy of the high energy transitions.

In the analysis of the results it is assumed that the strongest high energy transitions are nearly pure dipole transitions which very likely have E1 character. The possibility that an intense high energy transition is preceded by a low energy transition from the capturing state is considered to be less probable than the inverse process. This is justified by the fact that there is a strong increase of transition probability with increasing gamma energy and the fact that at high excitation energies the level density is much greater than at low energies. Therefore all strong high energy transitions are assumed to proceed from the capturing state. The spin of the capturing state is known to be 3 (see section 4.3). The anisotropies of the possible pure dipole transitions can be calculated using the value of f_2 given in section 4.2. The results are as follows:

$$3 \rightarrow 2 \qquad W(0^\circ) - 1 = + \frac{9}{10} f_2 G_2^n = +0.304$$

$$3 \rightarrow 3 \qquad W(0^\circ) - 1 = - \frac{9}{8} f_2 G_2^n = -0.380$$

$$3 \rightarrow 4 \qquad W(0^\circ) - 1 = + \frac{3}{8} f_2 G_2^n = +0.127$$

It is known that the 6502.8 keV transition proceeds from the capturing state to the 4^+ level at 1314 keV[2]. The measured value of the anisotropy for this transition which is $+0.12 \pm 0.01$ compares very well with the calculated value for a $3 \rightarrow 4$ transition. The measured anisotropies of the high energy transitions are given in table 4.IV. The spins of the final levels can be concluded from the anisotropy measurements using the expected anisotropies given above. They are listed in column 5 of table 4.IV. Spin assignments which are only possible with rather large quadrupole contributions are not accepted. Small quadrupole admixtures for the accepted assignments, which are compatible with the measured anisotropies, are given in column 6 of table 4.IV. The parities were assigned on the basis of the assumed E1 character of the primary transitions.

b. Anisotropy and linear polarization of the low energy transitions.

The disorientation parameters G_k were calculated for the levels at 1314, 1510 and 1560 keV with the Monte-Carlo programme outlined in chapter II. The following parameters were used: a=15, $\Delta = 1.25$, $\sigma = 5$ and $J = I - \frac{1}{2} = 3$.

The continuum was thought to extend above 1.6 MeV. Weisskopf estimates were used to compare the probabilities of the different dipole and quadrupole transitions. The results are given in table 4.VI together with the

Table 4.VI.

Calculated values of the disorientation paramaters G_2 and G_4 for ^{143}Nd.

spin of final level	Monte Carlo programme		simplified programme with ν is 3	
	G_2	G_4	G_2	G_4
2^+	0.43 ± 0.02	0.04 ± 0.01	0.44	0.04
3^-	0.55 ± 0.02	0.11 ± 0.01	0.52	0.04
4^+	0.58 ± 0.02	0.14 ± 0.01	0.60	0.15

G_k parameters calculated with the more simple programme in which the number of gamma transitions, ν, in each cascade is kept fixed. Using these values of G_k the expected anisotropies and degrees of linear polarization of the 814 and 864 keV transitions were calculated as a function of the mixing parameter δ. The results of these calculations are given in fig. 4.5 and compared to the measured values of the anisotropy and degree of linear polarization. The errors given in table 4.VI are of a statistical nature. However there are additional errors related to the simpifying assumptions which were made. The total errors were assumed to be less than 10% for the G_2 parameters. The G_4 parameters may have somewhat larger errors but their influence on the analysis is rather small. The ranges of multipole mixtures which are compatible with the measured values of the anisotropy and degree of linear polarization are given in column 6 of table 4.VII.

6. The decay schemes of ^{144}Nd and ^{146}Nd

a. The decay scheme of ^{144}Nd.

A partial decay scheme of ^{144}Nd is given in fig. 4.6. Several of the energy levels have also been observed in other experiments. The energies of the levels at 696.5 and 1314.4 keV have been taken from ref. 6. The high energy gamma transition of 6502.8 ± 1.0 keV is known to proceed to the level at 1314.4 ± 0.1 keV. [2,20] The resulting neutron binding energy is 7817.2 ± 1.1 keV. Assuming that the other observed high energy transitions originate from the capturing state several energy levels are predicted. For levels above 2.5 MeV these are only given in fig. 4.6 if in addition the anisotropy

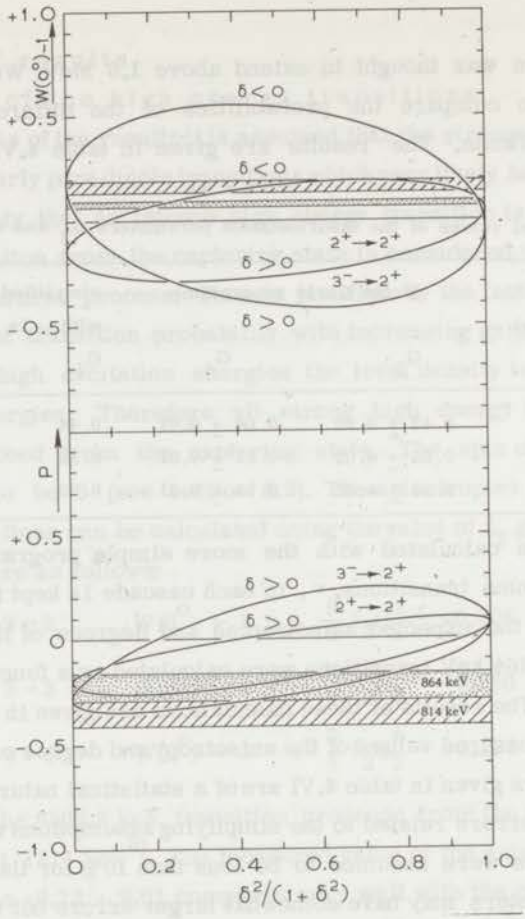

Fig. 4.5. Expected anisotropies and degrees of linear polarization for two low energy transitions in ^{144}Nd as a function of $\delta^2/(1+\delta^2)$.

of the corresponding high energy transitions could be measured. The position of most of the strongest transitions have been established by gamma-gamma coincidence measurements. Some transitions were put in the decay scheme on the basis of good energy fits. The energies of the low energy transitions were taken from ref. 2 and of the high energy transitions from table 4.III. Results which were obtained from the anisotropy and linear polarization measurements are given below for the individual energy levels.

696.5 keV. This level has been observed in several experiments. The 2^+ assignment has been based on a measurement of the directional correlation between gamma rays and scattered heavy ions, after Coulomb excitation [2]. The large negative anisotropy of the 696.5 keV ground state transition is in agreement with a $2^+ \rightarrow 0^+$ E2 transition.

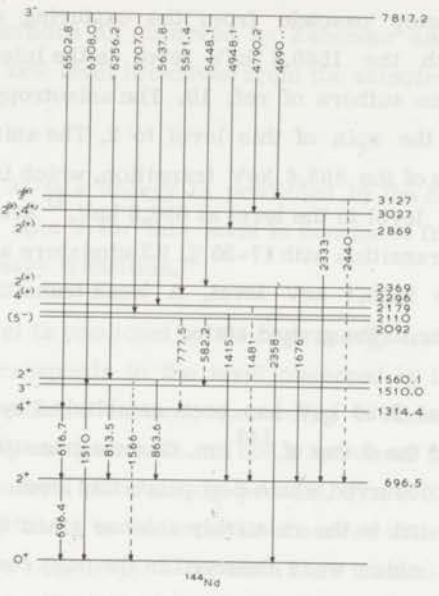

Fig. 4.6. Decay scheme of ^{144}Nd. Energies in keV.

1314.4 keV. The 4^+ assignment is based on directional correlation measurements of the 616.7-696.5 keV cascade [2]. The conversion coefficient of the 616.7 keV transition has been shown to be equal to the conversion coefficient expected for an E2 transition [2,9]. The large negative anisotropy of the 616.7 keV transition is in agreement with a $4^+ \rightarrow 2^+$ E2 transition.

1510.0 keV. This level is strongly excited by Coulomb excitation. It has been assigned as a 3^- level on the basis of the energy systematics of 3^- levels in even-even nuclei [2,18]. The anisotropy and degree of linear polarization of the 813.5 keV transition which is known to proceed from this level to the 2^+ level at 696.5 keV [4] are in agreement with a $3^- \rightarrow 2^+$ E1 transition. A weak transition of 6308 $\pm$ 5 keV which very likely proceeds from the capturing state to the 1510.0 keV level has been observed by Groshev [1]. The same transition may have been observed by Zehender and Fleischmann [19], who showed that there is a high energy transition which is coincident with a ground state transition of about 1510 keV. According to the authors of ref. 6 the 1510 keV ground state transition can also be observed in the decay of ^{144}Pm.

1560.1 keV. A two-step cascade from the capturing state to the level at 696.5 keV, in which the 1560.1 keV level is the intermediate state has been observed by the authors of ref. 19. The anisotropy of the 6256.2 keV transition restricts the spin of this level to 2. The anisotropy and degree of linear polarization of the 863.6 keV transition, which is known to proceed from the 1560.1 keV level to the level at 696.5 keV,[4] are only in agreement with a mixed M1-E2 transition with 17-30 % E2 admixture and exclude a negative parity for the 1560.1 keV level. A weak transition of 1566 ± 5 keV may be the cross-over to the ground state.

2092 keV. A level at 2093 keV has been established by the authors of ref. 4 and 5, who studied the decay of ^{144}Pm. Gamma transitions of 778.7, 582.6 and 302.0 keV were observed which depopulate this level. The first two transitions may correspond to the relatively intense transitions of 777.5 ± 0.6 and 582.2 ± 0.6 keV which were observed in the (n,γ) reaction[2]. A spin and parity 5^- have been suggested for this level by the authors of ref. 4.

2110 keV. The existence of this level has been established by the sum coincidence method [19]. The anisotropy of the rather weak high energy transition of 5707.0 keV could not be measured. The transition of 1415 ± 1 keV given in ref. 2 very likely corresponds to the transition observed by the authors of ref. 19 and proceeds from the 2110 keV level to the level at 696.5 keV.

2179 keV. A level at 2179 keV is predicted by the high energy transition of 5637.8 keV. The anisotropy of this rather weak transition could not be measured. The transition of 1481 ± 2 keV given in ref. 2 fits between the 2179 keV level and the level at 696.5 keV.

2296 keV. A level at this energy is predicted by the high energy transition of 5521.4 keV. The anisotropy of this transition is in agreement with a spin 4 for the 2296 keV level.

2369 keV. It has been shown by the authors of ref. 19 that there is a two-step cascade from the capturing state to the level at 696.5 keV and also one to the ground state in which the 2369 keV level is the intermediate level. The 2358 ± 20 keV and 1676 ± 6 keV transitions given in ref. 2 very likely

are the same transitions as observed by Zehender and Fleischmann [19]. A spin 2 for the 2369 keV level is derived from the anisotropy of the 5448.1 keV transition.

2869 keV. A level at this energy is predicted by the high energy transition of 4948.1 keV. A spin 2 for this level is concluded from the anisotropy of the 4948.1 keV primary transition.

3027 keV. This level is predicted by the high energy transition of 4790.2 keV and very likely corresponds to the level observed by the authors of ref. 19 with the sum coincidence method. According to these authors a two-step cascade from the capturing state to the 696.5 keV level in which the 3027 keV level is the intermediate state may be present. The 2333 ± 20 keV transition given in ref. 2 very likely is the same as observed with the sum coincidence method. The positive anisotropy of the 4790,2 keV transition restricts the spin of the 3027 keV level to 2 of 4.

3127 keV. A two-step cascade from the capturing state to the 2^+ level at 696.5 keV in which the 3127 keV level is the intermediate state, has been observed by the authors of ref. 19. This energy level may correspond to the energy level which is predicted on the basis of the high energy transition of 4690.1 keV and the second transition in the cascade possibly corresponds to the transition of 2440 ± 20 keV given in ref. 2. A spin 3 assignment for the 3127 keV level is derived from the negative anisotropy of the 4690.1 keV transition.

b. The decay scheme of ^{146}Nd.

A partial decay scheme of ^{146}Nd is given in fig. 4.7. The lowest excited state of this nucleus is at 453.7 ± 0.4 keV [10]. The high energy transition of 7112.0 ± 1.0 keV is known to proceed to this level [2,20] and the resulting neutron binding energy is 7565.7 ± 1.1 keV. Assuming that the other observed high energy transitions originate from the capturing state several other energy levels are predicted. Some of them have also been observed in other reactions and are indicated in fig. 4.7. The levels at 453.7, 1143, 1190, 1472, 1916 and 2516 keV have been observed in the decay of ^{146}Pr. The same levels with the exception of the level at 2516 keV have also been observed in the (n,α) reaction and the first three levels have been observed in the decay of ^{146}Pm. Levels

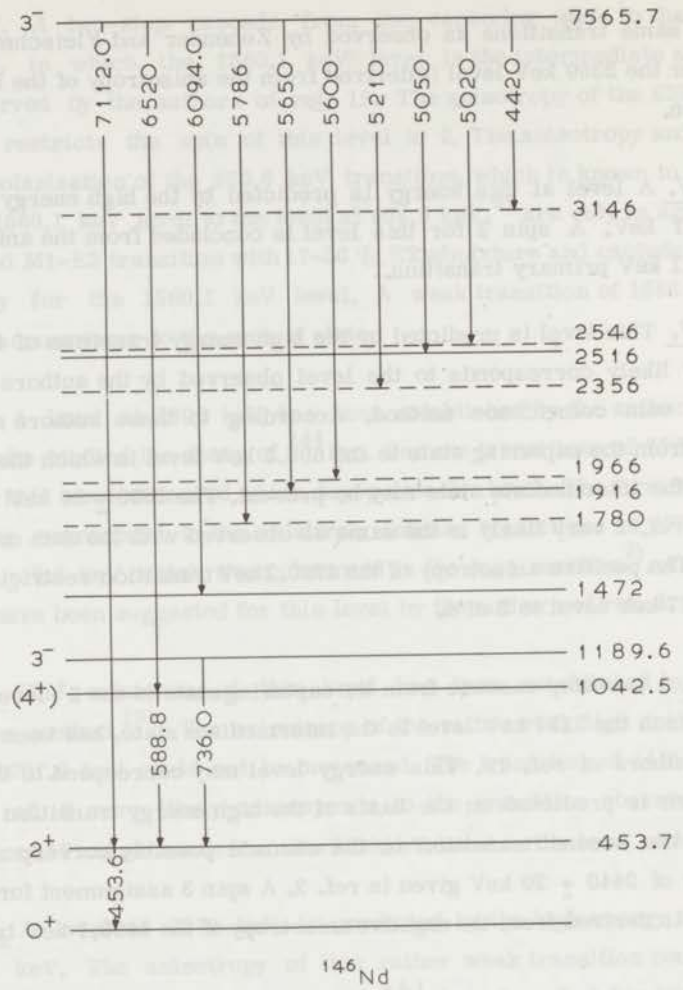

Fig. 4.7. Decay scheme of ^{146}Nd. Energies in keV.

which can only be derived on the basis of high energy neutron-capture gamma rays are indicated by dashed lines in fig. 4.7. The spins and parities of the energy levels and the energies of the low energy transitions were taken from ref. 2. The energies of the high energy transitions were taken from table 4.III.

REFERENCES

1. Groshev, L.V., Dvoretskii, V.N., Demidov, A.M. and Rachimov, A.S., I.V.Kurchatov Atomic Energy Institute report 1489 (1967).
2. Raman, S., Nuclear Data B2-1-47 (1967) and Martin, M.J., Nuclear Data B2-4-1 (1967).
3. Eissa, N.A., Berényi, D., Máthé, Gy., Varga, D., Rezanka, I. and Maly, L., Nuclear Phys. 100 (1967) 438.
4. Raman, S., Nuclear Phys. 117 (1968) 407.
5. Santhanam, S., Can. J. Phys. 46 (1968) 2181.
6. Barette, J., Monaro, S., Santhanam, S. and Markiza, S., Can. J. Phys. 46 (1968) 2189.
7. Hübel, H., Kesternich, W., Weigt, P. and Bodenstedt, E., Nuclear Phys. 107 (1968) 106.
8. Raman, S., Nuclear Phys. 107 (1968) 402.
9. Avotina, M.P., Grigorev, E.P., Zolotavin, A.V., Sergeev, V.O., Sovtsov, M.I., Vrzal, Ya. Lebedev, N.A., Liptak, Ya. and Urbanets, Ya., J.I.N.R. report 3471 (1967).
10. Taylor, H.W. and Kukoc, A.H., Nuclear Phys. 122 (1968) 425.
11. Meyer, H., Phil. Mag. 2 (1957) 521.
12. Blok, J., Shirley, D.A. and Stone, N.J., Phys. Rev. 143 (1966) 78.
13. Erickson, L.E., Phys. Rev. 143 (1966) 295.
14. Hughes, D.J. and Schwartz, R.B., B.N.L. report 325, second edition (1958).
15. Goldberg, M.D., Mughabghab, S.F., Purohit, S.N., Magurno, B.A. and May, V.M., B.N.L. report 325, second edition (1966).
16. Kvitek, I. and Popov, Yu.P., J.E.T.P. Letters 5 (1968) 301.
17. Diddens, A.N., Thesis, University of Groningen 1957.
18. Hansen, O. and Nathan, O., Nuclear Phys. 42 (1963) 197.
19. Zehender, O. and Fleischmann, R., Zeitsch. Phys. 188 (1965) 93.
20. Mattauch, J.H.E., Thiele, W. and Wapstra, A.H., Nuclear Phys. 67 (1965) 1.

CHAPTER V

NEUTRON-CAPTURE GAMMA-RAY SPECTRA FROM ^{147}Sm, ^{149}Sm AND ^{152}Sm INCLUDING ANISOTROPY MEASUREMENTS OF NEUTRON-CAPTURE GAMMA RAYS FROM ALIGNED ^{149}Sm NUCLEI

1. Introduction

Natural samarium consists of several stable isotopes of which ^{147}Sm and ^{149}Sm can be oriented in single crystals of cerium (samarium) magnesium double nitrate. In the nuclear orientation experiments a sample containing natural samarium was used and although the cross-section of ^{149}Sm is very large it was realized that one or more of the observed weak gamma transitions could actually be related to capture in one of the other samarium isotopes. It was therefore decided to compare the capture gamma-ray spectrum of natural samarium with the spectra of samples enriched in the isotopes ^{152}Sm and ^{147}Sm. The isotope ^{152}Sm has the largest cross-section following ^{149}Sm and a study of the capture gamma-ray spectrum of ^{147}Sm is of interest for future alignment experiments. The anisotropy of capture gamma rays from aligned ^{149}Sm nuclei was measured mainly in the direction of nuclear orientation. By combining the results of the anisotropy measurements with the available electron conversion data, the spins of some energy levels were reestablished and several new spin values were obtained.

Partial decay schemes are given for the nuclei ^{150}Sm, ^{148}Sm and ^{153}Sm in which the obtained results are combined with information from several other experiments. The energy level scheme of ^{150}Sm has been studied using a variety of methods and reactions. The neutron-capture gamma-ray spectrum of ^{149}Sm has been investigated by several authors. Precision gamma-ray measurements have been performed by Smither[1] with a bent-crystal spectrometer and by Groshev e.a.[2] with a magnetic Compton spectrometer. The electron conversion spectrum has been measured by these authors and also by Elze [3]. The directional correlation and coincidences of

several gamma transitions have been investigated by Smither[1] and by Cojocaru e.a.[4]. Two-step cascades from the capturing state to the levels at 334 and 773 keV have been observed by Zehender and Fleischmann[5]. Some energy levels have been established with $\beta - \gamma$ coincidences by Govor and Ivanov[6]. Many energy levels of ^{150}Sm below 2.5 MeV together with their spins and parities have also been found in decay studies. The electron capture decay of ^{150}Eu (13 h) and ^{150}Eu (5 y) has been studied by Guttman e.a.[7] and by Kugel e.a.[8]; Gove an O'Kelly[9] have investigated the β-decay of ^{150}Pm. By Coulomb excitation many energy levels of the ^{150}Sm nucleus have been observed by Seaman e.a.[10], Keddy e.a.[11] and by Veje e.a.[12]. Finally many particle reactions in which ^{150}Sm is the final nucleus have been studied. The (α,xn) reaction, which has been studied by Morinaga[13], revealed some energy levels. The (d,p) and (p,p') reactions have been investigated by Kenefick and Sheline[14]. The (t,p) reaction has been studied by Bjerregaard e.a.[15]. Information on the spins of some levels has been obtained by measuring the directional distribution of tritons in the (p,t) reaction studied by Ishizaki e.a.[16] and of deuterons in the (d,d') reaction which was studied by Veje e.a.[12].

Information on the energy levels of ^{148}Sm including their spins and parities can be found in ref. 10 - 14 and 16. The data partly obtained from these references and partly from decay studies of ^{148}Pm and ^{148}Eu have been compiled in the Nuclear Data Sheets[17]. The electron conversion coefficients of gamma transitions observed in the β-decay of ^{148}Pm have recently been measured by Avotina e.a.[18].

Many energy levels of the ^{153}Sm nucleus have been found in the (d,p) reaction which has been studied by Kenefick and Sheline[19]. The β-decay of ^{153}Pm was studied by Kotajima[20]. The neutron-capture gamma-ray spectrum and corresponding electron-conversion spectrum have been measured by Smither e.a. Some preliminary results of their measurements are given in ref. 21 and 22.

2. Alignment of samarium nuclei

The samarium nuclei were aligned in single crystals of $Ce_2Mg_3(NO_3)_{12}.24\ D_2O$ in which part of the Ce-ions was replaced by Sm-ions. Most of the water of crystallization was replaced by D_2O in order to reduce the scattering of neutrons in the crystal. Two samples each weighing about 20 g were used.

In one of them (sample I) about 7 % of the Ce-ions was replaced by samarium. In this sample almost complete alignment could be obtained immediately after demagnetization. In the other sample (sample II) about 20 % of the Ce-ions was replaced by samarium. It was used to measure the anisotropy of the much weaker high energy transitions. A considerable alignment could still be reached in it.

The magnetic properties of the individual ^{149}Sm ions in the isomorphous SmMg double nitrate crystals can be described with the effective-spin Hamiltonian[23]:

$$\mathcal{H} = g_{\parallel}\mu_B H_z S_z + g_{\perp}\mu_B (H_x S_x + H_y S_y) + A S_z I_z + B(S_x I_x + S_y I_y). \qquad 5.1$$

For ^{149}Sm the following constants are known: The nuclear spin $I = 7/2$, the effective electron spin $S = \frac{1}{2}$, the splitting factors are $g_{\parallel} = -0.76$ and $g_{\perp} = 0.40$, the hyperfine splitting constants are $A/k = 0.0413$ K and $0 > B/k > -0.0158$ K. The numerical values are from ref. 23 and the signs from ref. 24 and 25. The orientation parameters f_2 and f_4 were calculated for ^{149}Sm as a function of temperature using the value of A/k mentioned above in combination with $B/k = -0.0158$ K and $B/k = 0$ K respectively. The results of this calculation are shown in fig. 5.1. Starting from an initial temperature of 1.0 K

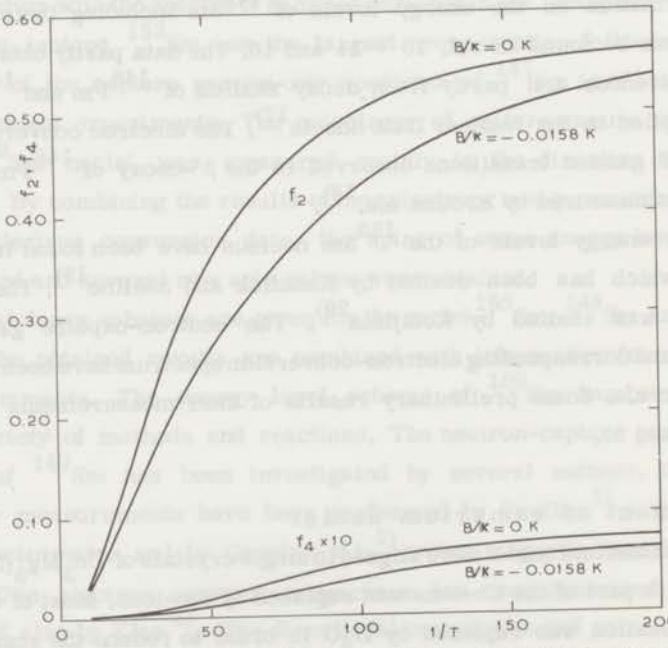

Fig. 5.1. Calculated curves of f_2 and f_4 in samarium magnesium double nitrate as a function of temperature.

and a field of 12 kOe a final temperature of about 0.01 K could be reached (see section 5.4.c). The temperature increased rapidly during the time in which the data were taken. This increase in temperature was observed by measuring the anisotropy of the intense 440 keV transition as a function of time. In fig. 5.2 the results are shown for sample II. As a consequence all measured anisotropies and orientation parameters are averaged values. The measuring time was 11 minutes for each sample. The crystals were mounted in such a way that the c-axes, along which the ^{149}Sm nuclei tend to align, were parallel to the axis of the cryostat tail.

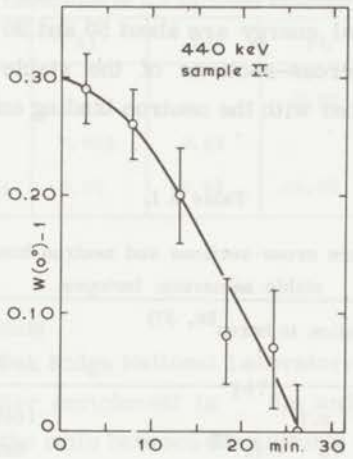

Fig. 5.2. Anisotropy of the 440 keV transition as a function of time for sample II.

3. Neutron capture by samarium

The total cross-section of natural samarium at 0.047 eV, the neutron energy used in the alignment experiments, is 6900 barns. Only 48 barns are due to scattering[26]. At the above-mentioned energy 99 % of the cross-section is due to ^{149}Sm and most of it is related to the 0.0976 eV resonance. The next resonance, at 0.873 eV, contributes at most 14 barns. A careful comparison of the cross-section of samarium with the Breit-Wigner formula fitted to the 0.0976 eV resonance showed that a negative resonance (bound state) of ^{149}Sm also contributes to the thermal neutron capture. The cross-section in the thermal region has been estimated to be $48/\sqrt{E}$[27] or $105\sqrt{E}$[28] barns (E in eV). This means that 3 to 7 % of the cross-section at 0.047 eV is due to this resonance. At 0.125 eV its contribution is reduced by a factor 1.6. This difference was used to detect possible gamma rays related to this bound state (see

section 5.4.d).

The spin of the 0.0976 eV resonance has been shown to be 4 in a number of different experiments[29-32]. A spin 4 has also been assigned to the next three resonances[31]. The spin of the bound state is 3 as has been obtained by studying the $^{149}Sm(n,\alpha)^{146}Nd$ reaction at various neutron energies[33-36].

The contribution of ^{147}Sm and ^{152}Sm to the total cross-section is very low. The spin of the capturing state of ^{153}Sm will be $\frac{1}{2}$ since the spin of the target nucleus is zero. The spins of the first two resonances of ^{147}Sm, observed at 3.4 and 18.3 eV, have been determined to be 3 and 4, respectively[37,38]. The contributions of these two resonances to the capture cross-section of ^{147}Sm at thermal energy are about 50 and 30 % respectively. The thermal neutron-capture cross-sections of the stable samarium isotopes are given in table 5.I together with the neutron binding energies.

Table 5.I.

Thermal neutron-capture cross-sections and neutron-binding energies of stable samarium isotopes.

isotope	cross-section in barns[26, 37]	binding energy[47] in KeV
^{144}Sm	0.7	10460 ± 80
^{147}Sm	75 ± 11[45]	6325 ± 18
^{148}Sm	4.73 ± 0.77[46]	8142 ± 5
^{149}Sm	41000 ± 2000	5846.2 ± 4.8
^{150}Sm	102 ± 5	7981.9 ± 2.7
^{152}Sm	210 ± 10	8224 ± 16
^{154}Sm	5.5 ± 1.1	7904 ± 12

4. Experimental results

a. Neutron-capture gamma-ray spectra of natural samarium and of isotopically enriched samarium samples.

The isotopic and spectrographic analyses of the enriched samarium samples, used in the experiment, are shown in table 5.II together with the isotopic composition of natural samarium. All the samples were in the form of Sm_2O_3. Two of the enriched samples, ^{147}Sm(I) and ^{152}Sm, were obtained on loan from the U.K.A.E.R.E. at Harwell. A second sample, enriched in ^{147}Sm,

Table 5.II

Isotopic composition of the samarium samples in per cents.

sample	weight	^{144}Sm	^{147}Sm	^{148}Sm	^{149}Sm	^{150}Sm	^{152}Sm	^{154}Sm
^{147}Sm(I)	100 mg	0.13	92.52	5.14	1.28	0.26	0.47	0.26
^{152}Sm	100 mg	0.03	0.17	0.13	0.19	0.16	98.55	0.76
natural	2 mg	3.09	14.97	11.24	13.83	7.44	26.72	22.71
^{147}Sm(II)	115 mg	<0.10	97.93	0.84	0.50	0.17	0.35	0.21

Impurities of the enriched samples in per cents.

sample	Al	Mg	Pb	Si	Fe
^{147}Sm(I)			0.02	0.002	
^{152}Sm	0.002	0.02		0.06	0.01
^{147}Sm(II)	<0.05	<0.01	<0.02	<0.02	<0.02

was obtained from Oak Ridge National Laboratory. This sample, ^{147}Sm(II) in table 5.II has a better enrichment in ^{147}Sm and contains considerably less ^{149}Sm. In addition the ratio between the amounts of ^{148}Sm and ^{149}Sm in this sample is only increased by a factor two as compared to the natural composition, while in the ^{147}Sm(I) sample this ratio is increased by a factor five. The influence of ^{150}Sm can also be observed since the ratio between ^{150}Sm and ^{149}Sm is 2 to 3 times less in the enriched ^{147}Sm samples.

Relevant parts of the spectra obtained with the enriched samples from Harwell and from a sample of natural samarium are shown in fig. 5.3 to 5.7. They were obtained with the 6.4-cc Philips detector. Each part of the high energy spectra covers 512 channels of the 4096-channel analyser. Not all channels were plotted: in regions where there are no peaks visible each second point is given only. Double-escape peaks are indicated with a double prime, single escapes with a single prime and photopeaks are not indicated. Some of the peaks are due to neutron capture in the material that surrounds the target. They are marked with Bgr or with Fe if they are due to iron. The second ^{147}Sm sample showed a spectrum very similar to the one measured

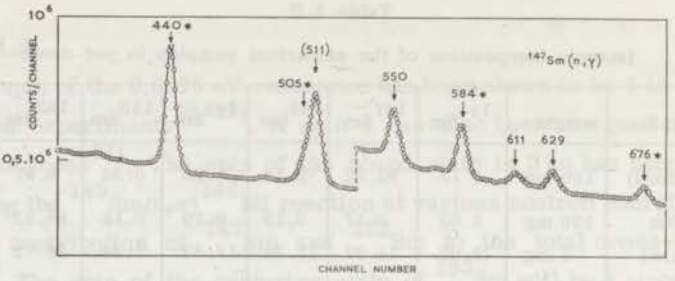

Fig. 5.3. Low energy part of the neutron-capture gamma-ray spectrum from ^{147}Sm. Energies in keV. Peaks with an asterisk are due to capture in ^{149}Sm.

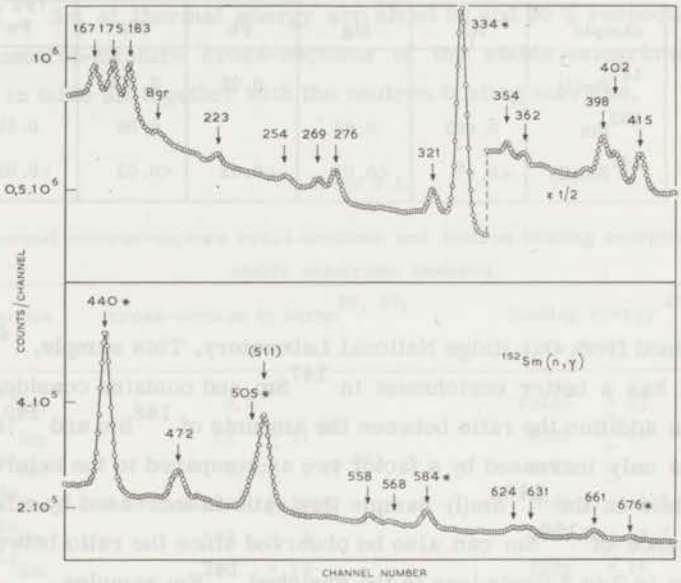

Fig. 5.4. Low energy part of the neutron-capture gamma-ray spectrum from ^{152}Sm. Energies in keV. Peaks with an asterisk are due to capture in ^{149}Sm.

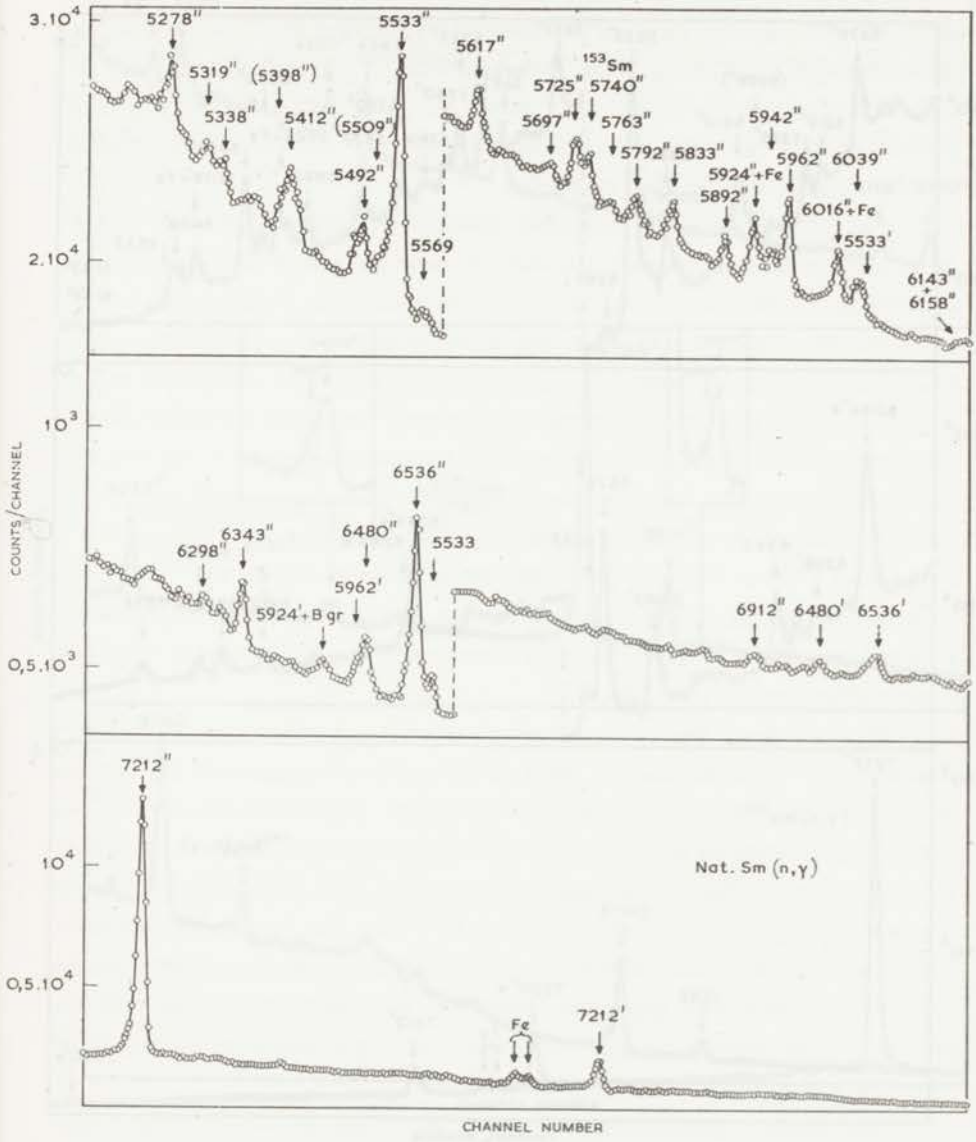

Fig. 5.5. High energy part of the neutron-capture gamma-ray spectrum from natural samarium. Energies are given in keV.

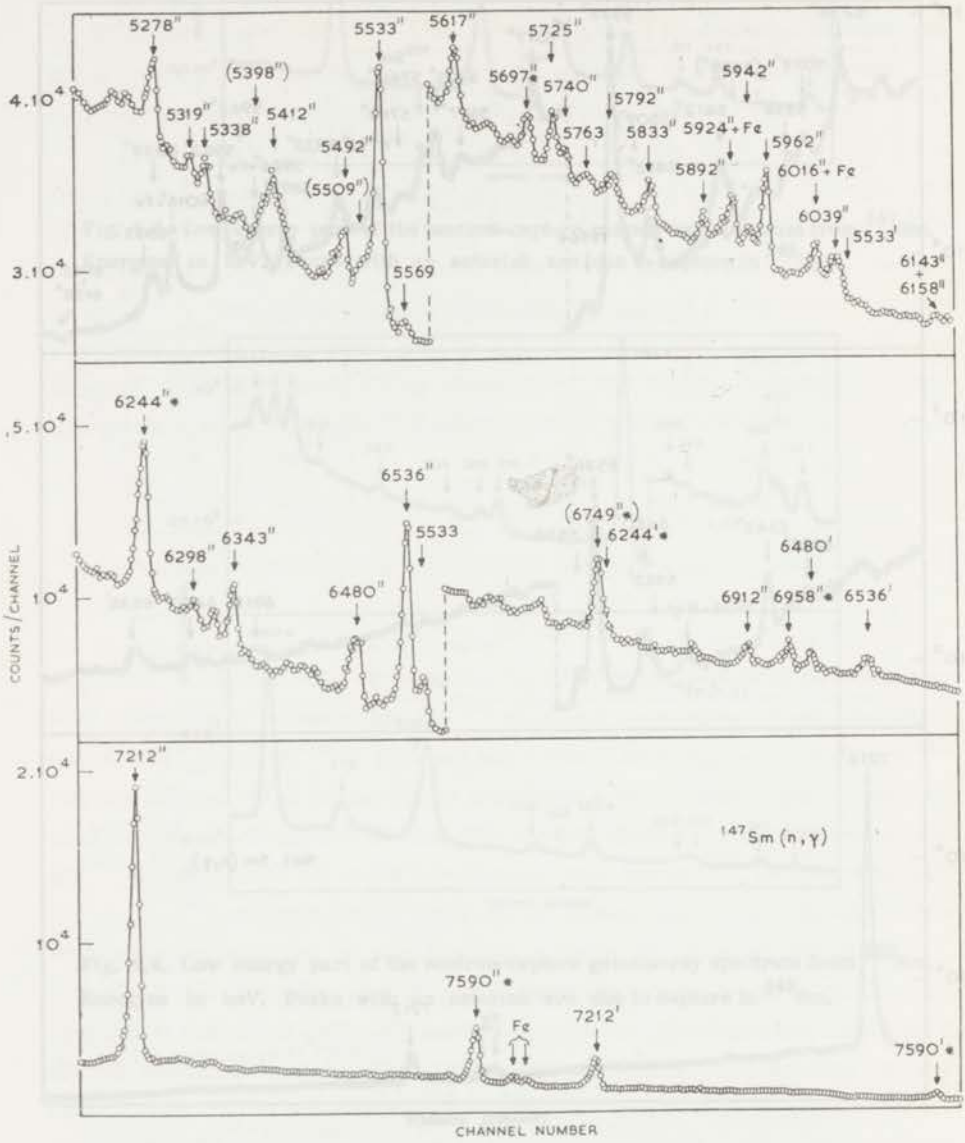

Fig. 5.6. High energy part of the neutron-capture gamma-ray spectrum from ^{147}Sm. Energies are given in keV.

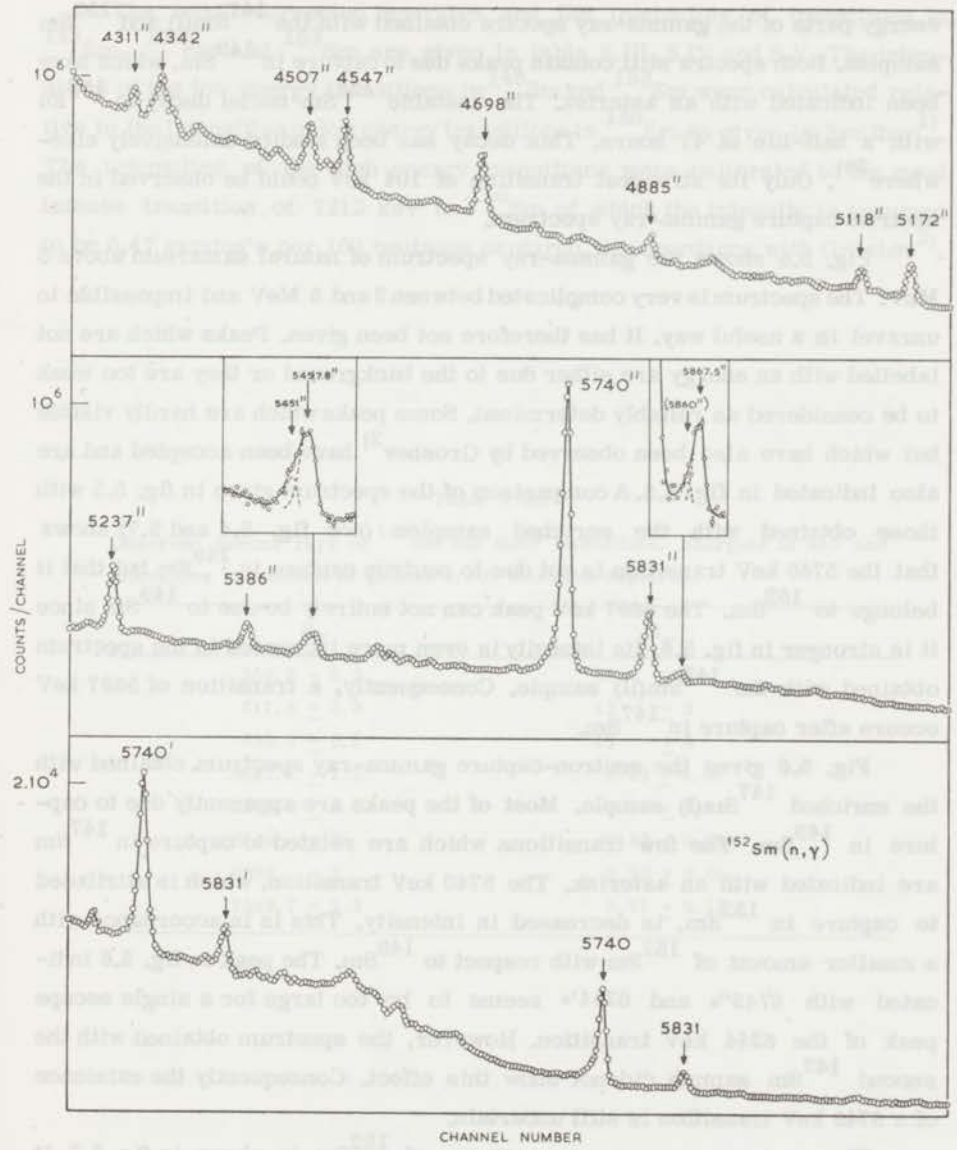

Fig. 5.7. High energy part of the neutron-capture gamma-ray spectrum from ^{152}Sm. Energies are given in keV.

with the ^{147}Sm(I) sample obtained from Harwell. Fig. 5.3 and 5.4 show low energy parts of the gamma-ray spectra obtained with the ^{147}Sm(I) and ^{152}Sm samples. Both spectra still contain peaks due to capture in ^{149}Sm, which have been indicated with an asterisk. The unstable ^{153}Sm nuclei decay to ^{153}Eu with a half-life of 47 hours. This decay has been studied extensively elsewhere[39]. Only its strongest transition of 104 keV could be observed in the neutron-capture gamma-ray spectrum.

Fig. 5.5 shows the gamma-ray spectrum of natural samarium above 5 MeV. The spectrum is very complicated between 2 and 5 MeV and impossible to unravel in a useful way. It has therefore not been given. Peaks which are not labelled with an energy are either due to the background or they are too weak to be considered as reliably determined. Some peaks which are hardly visible but which have also been observed by Groshev[2] have been accepted and are also indicated in fig. 5.5. A comparison of the spectrum given in fig. 5.5 with those obtained with the enriched samples (see fig. 5.6 and 5.7) shows that the 5740 keV transition is not due to neutron capture in ^{149}Sm but that it belongs to ^{152}Sm. The 5697 keV peak can not entirely be due to ^{149}Sm since it is stronger in fig. 5.6. Its intensity is even more increased in the spectrum obtained with the ^{147}Sm(II) sample. Consequently, a transition of 5697 keV occurs after capture in ^{147}Sm.

Fig. 5.6 gives the neutron-capture gamma-ray spectrum obtained with the enriched ^{147}Sm(I) sample. Most of the peaks are apparently due to capture in ^{149}Sm. The few transitions which are related to capture in ^{147}Sm are indicated with an asterisk. The 5740 keV transition, which is attributed to capture in ^{152}Sm, is decreased in intensity. This is in accordance with a smaller amount of ^{152}Sm with respect to ^{149}Sm. The peak in fig. 5.6 indicated with 6749"* and 6244'* seems to be too large for a single escape peak of the 6244 keV transition. However, the spectrum obtained with the second ^{147}Sm sample did not show this effect. Consequently the existence of a 6749 keV transition is still uncertain.

The capture gamma-ray spectrum of ^{152}Sm is shown in fig. 5.7. It turned out to be a rather clean spectrum showing at most minor traces of ^{149}Sm. The assigned peaks are attributed to neutron capture in ^{152}Sm. Peaks which are not marked are either due to ^{150}Sm, to the background or they are too small for a reliable determination. The peaks at 5457.8 and 5867.5 keV are considerably broader than the other peaks. This is very likely due to

weak transitions of 5451 and 5860 keV as is indicated in the inserts.

The recoil-corrected energies and the intensities of transitions in ^{148}Sm, ^{150}Sm and ^{153}Sm are given in table 5.III, 5.IV and 5.V. The intensities of the low energy transitions in ^{148}Sm and ^{153}Sm were calculated relative to the intensities of low energy transitions in ^{150}Sm as given by Smither[1]. The intensities of the high energy transitions were calibrated to the most intense transition of 7212 keV in ^{150}Sm of which the intensity is assumed to be 0.47 gamma's per 100 neutrons captured, in accordance with Groshev[2].

Table 5.III.

Observed gamma rays of ^{148}Sm and their intensities. Energies in keV and intensities in number of gamma's/100 neutrons captured.

E_γ	I_γ
550.3 ± 0.3	50 ± 9
611.5 ± 0.3	13 ± 3
630.0 ± 0.3	18 ± 4
5697.1 ± 1.5	0.29 ± 0.06
6244.0 ± 1.5	0.97 ± 0.14
(6749 ± 2)	(0.40 ± 0.09)
6958 ± 2	0.20 ± 0.05
7589.7 ± 1.1	0.71 ± 0.13

Table 5.IV.

Observed high energy gamma-rays of ^{150}Sm and their intensities. Energies in keV and intensities in number of gamma's/100 neutrons captured. Values between parentheses are uncertain and are possibly partly due to single escape peaks.

present work		Groshev	
E_γ	I_γ	E_γ	I_γ
7212.0 ± 1.1	0.47	7210	0.47
6912 ± 1.5	0.010 ± 0.003	6912	0.011
		6623	0.008
6535.9 ± 1.2	0.13 ± 0.01	6532	0.12
6479.9 ± 1.5	0.040 ± 0.006	6475	0.043
6342.8 ± 1.5	0.033 ± 0.006	6339	0.030
6298.4 ± 1.5	0.010 ± 0.003	6304	0.013
6158 ± 5	0.018 ± 0.004	6160	0.023
6143 ± 5	0.010 ± 0.004	6143	0.010
6039 ± 3	0.015 ± 0.005	6031	0.03
6016.3 ± 3.5	0.060 ± 0.010	6013	0.06
5961.7 ± 1.5	0.12 ± 0.02	5958	0.16
(5942 ± 2	0.040 ± 0.015)	----	----
5923.6 ± 1.5	0.086 ± 0.015	5923	0.07
5891.8 ± 1.5	0.044 ± 0.008	5893	0.03
		5863	0.015
5833 ± 2	0.048 ± 0.006	5827	0.04
5792 ± 4	0.030 ± 0.006	5787	0.03
(5763 ± 3	0.012 ± 0.002)	----	----
5725 ± 3	0.070 ± 0.020	5721	0.10
5697 ± 3	0.019 ± 0.003	5692	0.02
5617.0 ± 1.5	0.060 ± 0.008	5609	0.07
(5569 ± 4	0.010 ± 0.004)	----	----
5532.5 ± 1.5	0.38 ± 0.05	5526	0.40
5509+	0.03	5509	0.06
5492 ± 2	0.10 ± 0.01	5485	0.14
5412+	0.13 ± 0.02	5412	0.11
5398+		5398	0.05

+) Energy values of L. V. Groshev.

Tabel 5.V.

Observed gamma-rays of ^{153}Sm and their intensities. Energies in keV and intensities in number of gamma's/100 neutrons captured. Energy values with an asterisk and their corresponding intensities are from ref. 48.

E_γ	I_γ	E_γ	I_γ
5867.5 ± 1.0	0.09 ± 0.02	567.9 ± 1	0.56 ± 0.11
(5860)		558.2 ± 0.5	1.3 ± 0.3
5831.2 ± 0.4	0.74 ± 0.08	472.2 ± 0.4	2.5 ± 0.4
5739.7 ± 0.4	4.1 ± 0.4	414.9 ± 0.4	2.7 ± 0.4
5457.8 ± 1.0	0.45 ± 0.05	402.0 ± 1	1.8 ± 0.3
5451 ± 2		362.0 ± 0.4	0.27 ± 0.10
5386.6 ± 1.0	0.26 ± 0.05	354.3 ± 0.4	0.44 ± 0.20
5237.2 ± 1.0	0.79 ± 0.08	321.0 ± 0.5	2.1 ± 0.4
5172.0 ± 1.0	0.42 ± 0.05	276 ± 1	3.0 ± 0.6
5117.7 ± 1.5	0.20 ± 0.04	269 ± 1	2.0 ± 0.4
4884.8 ± 1.5	0.19 ± 0.05	254 ± 1	1.1 ± 0.5
4697.9 ± 1.0	0.74 ± 0.09	223 ± 1	0.24 ± 0.10
4546.8 ± 1.0	0.60 ± 0.07	182.901*	10
4506.6 ± 1.0	0.60 ± 0.07	175.365*	10
4341.5 ± 1.5	0.87 ± 0.09	166.646*	5
4310.7 ± 1.5	0.28 ± 0.05	127.300*	5
660.6 ± 0.8	1.2 ± 0.3	119.770*	5
630.6 ± 1	2.2 ± 0.5	90.875*	1.2
623.6 ± 1		35.847*	1.6

b. Anisotropy of the directional distribution.

The total background at each peak was determined by fitting a parabola through suitably chosen intervals of points on the left and right of each peak. The areas, S, of the peaks were obtained after subtraction of the background. The experimental anisotropy, which is defined as [S(0.01 K) - S(1 K)]/S(1 K), was calculated for each peak separately. For some transitions, of which the intensity is very low or which coincide with peaks in the background, only the difference in area at 0.01 K and 1 K could be determined experimentally. Using the intensities given in the literature[1,2] and in table 5.IV the areas

at 1 K of these transitions were calculated from the areas of the more intense peaks. In the analysis of the high energy part of the spectra it was necessary to correct many of the areas under the peaks for the influence of single escape peaks of other transitions and for background peaks. Fig 5.8 shows as an example a part of the high energy spectrum measured at the two different temperatures. Large negative anisotropies of about 30–40 % are easily recognized

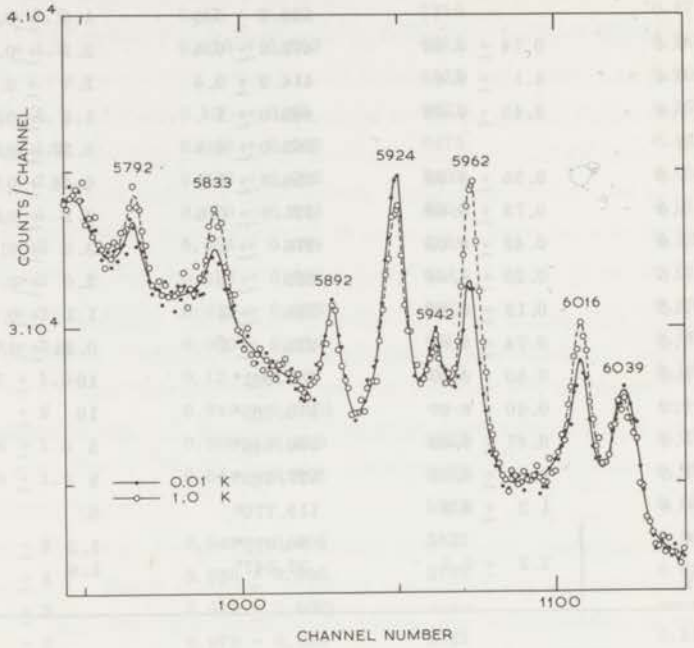

Fig. 5.8. A part of the high energy spectrum measured with the samarium sample at 1.0 and 0.02 K.

for the transitions of 5792, 5833 and 5962 keV. The anisotropies of the 5924 and 6016 keV transitions had to be corrected for the influence of single escape peaks and the background of iron. The anisotropies of the high energy transitions are given in table 5.VI. A part of the low energy spectrum together with the difference of the spectra at 0.01 and 1 K is shown in fig. 5.9. The anisotropies of the low energy transitions obtained with sample I are given in the second column of table 5.VII.

Table 5. VI.

The energies and measured anisotropies of the high energy capture gamma rays from ^{149}Sm nuclei, aligned in sample II, are given in column 1 and 2. The conversion coefficients and tentative multipole assignments can be found in the next two columns. The energies of the final levels and the spins which can be concluded from the anisotropy measurements assuming pure dipole transitions, are given in column 5 and 6. Column 7 gives the possible quadrupole admixtures compatible with the anisotropies.

E_γ in keV	anisotropy $W(0^\circ)-1$	conversion coefficient	tentative character	final level in keV	spin of final level	possible quadrupole admixture in %
7212.0	-0.35±0.01	(3.8±0.2)(-5)	E1	773.4	4^+	
6535.9	-0.35±0.03	(4.6±0.7)(-5)	E1	1449.3	4^+	<0.8 (or >46)
6479.9	+0.18±0.07	(3.6±1.4)(-5)	E1	1504.7	3^+, 5^+	<1
6342.8	-0.37±0.08	-	E1*	1642.7	4^+	<6 (or >27)
6298.4	-0.50±0.20	-	-	1684.2	(3, 4)	
6158	-0.20±0.10	-	E1*	1822	3^+, 4^+	
6143	+0.27±0.19	-	-	1843.6	-	
6039	-	(1.6±0.8)(-4)	M1	1951	2^-, 3^-, 4^-, 5^-	
6016.3	-0.36±0.09	(7.3±2.6)(-5)	E1, M1	1971.9	4	<6 (or >27)
5961.7	-0.36±0.03	(6.0±1.1)(-5)	E1	2021.5	4^+	<0.8 (or >43)
5923.6	+0.23±0.07	(5.8±1.4)(-5)	E1	2062.9	3^+, 5^+	<2
5891.8	+0.02±0.07	(3.5±1.9)(-5)	E1	2094	5^+	
5833	-0.30±0.07	-	E1*	2153.3	4^+	<4.5 (or >47)
5792	-0.39±0.15	(1.5±1.0)(-4)	M1, E1	2191.2	4	<57
5725	-0.31±0.07	(4 ±4)(-4)	E1, M1	2260	4	<4 (or >46)
5697	+0.53±0.23	(1.1±0.4)(-4)	M1	2288	-	
5617.0	+0.29±0.09	(6.0±1.2)(-5)	E1	2368	3^+, 5^+	<0.9
5532.5	+0.245±0.015	(5.4±0.9)(-5)	E1	2453	3^+	<0.1
5492	+0.17±0.09	(5.2±0.8)(-5)	E1	2493	3^+, 5^+	<1.5
5338	+0.14±0.08	(7.3±2.0)(-5)	E1 (M1)	2647	$3^{(+)}$, $5^{(+)}$	<1.5

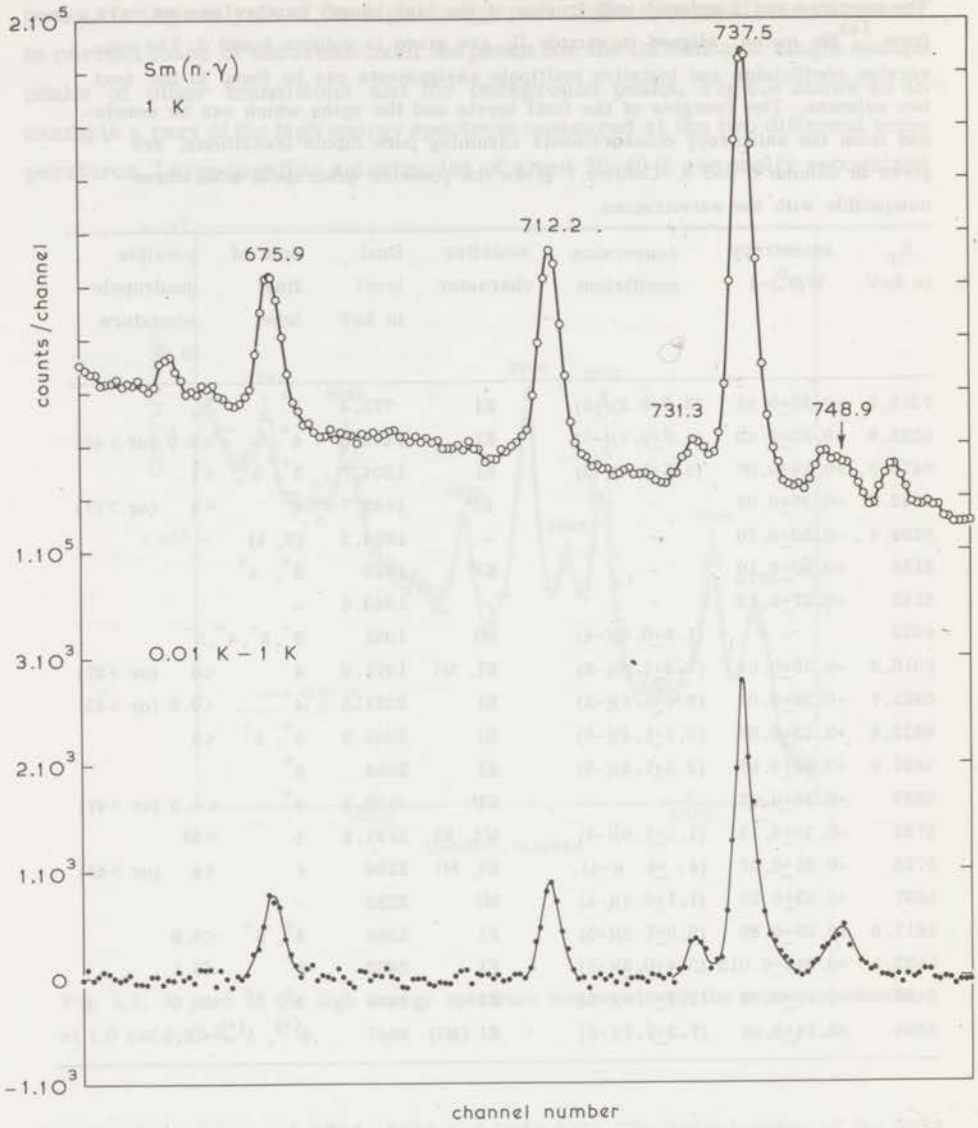

Fig. 5.9. A part of the low energy spectrum measured with the samarium sample at 1.0 K and the difference of the spectra measured with the sample at 0.01 and 1.0 K.

Table 5. VII.

The energies and measured anisotropies of the low energy capture gamma rays from ^{149}Sm nuclei aligned in sample I are given in column 1 and 2. For each possible transition, given in column 3, the corresponding ranges of multipole mixtures and K-conversion coefficients compatible with the anisotropy are given in column 4 and 5. If the experimental K-conversion coefficient in column 6 is in the range given in column 5 the transition is accepted and marked with an asterisk in column 7.

E_γ in keV	anisotropy $W(0^\circ)-1$	transition	multipole admixture		range of K-conversion coefficient	experimental K-conversion coefficient		remarks
333.9	-0.298±0.005	$2^+ \to 0^+$	100%E2					
403.0	-0.38 ±0.3	$4^+ \to 2^+$	96-100%E2	0-4%M3	0.018-0.030	0.020±0.003	*	Probably pure E2. Composite peak with 406.6 keV which has no anisotropy
		$4^+ \to 2^+$	0-4%E2	96-100%M3	0.31-0.32			
439.5	-0.393±0.005	$4^+ \to 2^+$	100%E2					
486.0	+0.40 ±0.05	$2^+ \to 3^-$	1-92%E1	8-99%M2	0.0086-0.061	0.0072±0.0043	*	
		$3^+ \to 3^-$	9-36%E1	64-91%M2	0.041-0.057			
		$4^+ \to 3^-$	98-100%E1	0-2%M2	0.0039-0.0055		*	
			4-12%E1	88-96%M2	0.055-0.060			
		$4^+ \to 5^-$	88-99%E1	1-12%M2	0.0045-0.011		*	
			0-6%E1	94-100%M2	0.060-0.062			
		$5^+ \to 5^-$	0-58%E1	42-100%M2	0.028-0.062			
505.6	-0.40 ±0.05	$3^+ \to 4^+$	32-78%M1	22-68%E2	0.012-0.015	0.012±0.002	*	
		$3^- \to 4^+$	38-72%E1	28-62%M2	0.017-0.034		(*)	
		$4^+ \to 4^+$	40-100%M1	0-60%E2	0.013-0.017		*	
		$4^- \to 4^+$	40-100%E1	0-60%M2	0.0034-0.033		*	
		$5^+ \to 4^+$	75-86%M1	14-25%E2	0.015-0.016		*	

Table 5. VII (continued)

E_γ in keV	anisotropy $W(0^o)-1$	transition	multipole admixture δ		range of K-conversion coefficient	experimental K-conversion coefficient		remarks
			6-15%M1	85-94%E2	0.010-0.011		*	
		$5^- \to 4^+$	75-86%E1	14-25M2	0.010-0.016		*	
			6-15%E1	85-94%M2	0.045-0.049			
		$6^+ \to 4^+$	100%E2		0.01		*	
558.2	-0.16 ±0.03	$3^+ \to 3^+$	91-98%M1	2-9%E2	0.013-0.014	0.014±0.003	*	
			9-21%M1	79-91%E2	0.008-0.009			
		$5^+ \to 3^+$						Anisotropy of a $5^+ \to 3^+$E2 transition is -0.39
571.2	+0.33 ±0.08	$4^+ \to 3^-$	97-100%E1	0-3%M2	0.0027-0.037	0.0040±0.0007		
			3-9%E1	91-97%M2	0.034-0.036			
584.3	+0.290±0.010	$3^- \to 4^+$	93-99%E1	1-7%M2	0.0029-0.0048	0.0029±0.0005	*	Anisotropy of a $4^- \to 4^+$E1 transition is negative
			0-2%E1	98-100%M2	0.034-0.035			
		$5^- \to 4^+$	99-100%E1	0-1%M2	0.0026-0.0029		*	
			1-5%E1	95-99%M2	0.033-0.035			
675.9	+0.269±0.015	$4^+ \to 4^+$	0-45%M1	55-100%E2	0.0049-0.0065	0.017±0.003		EO admixture
712.2	+0.195±0.014	$1^- \to 2^+$	4-96%M1	4-96%M2	0.0025-0.020	0.0086±0.0014	*	
		$1^+ \to 2^+$	0-95%M1	5-100%E2	0.0044-0.0064		*	
		$2^- \to 2^+$	58-75%E1	25-42%M2	0.0066-0.0098		*	
			1-11%E1	89-99%M2	0.019-0.021			
		$2^+ \to 2^+$	52-74%M1	26-48%E2	0.0060-0.0066		*	
			2-12%M1	88-98%E2	0.0044-0.0047		(*)	
		$3^+ \to 2^+$	98-100%M1	0-2%E2	0.0074-0.0075		*	
			2-5%M1	95-98%E2	0.0042-0.0044		(*)	
		$3^- \to 2^+$	98-100%E1	0-2%M2	0.0018-0.0021			
			2-5%E1	95-98%M2	0.02			

Table 5. VII (continued)

E_γ in keV	anisotropy $W(0^o)-1$	transition	multipole admixture		range of K-conversion coefficient	experimental K-conversion coefficient		remarks
731.3	+0.40 ±0.10	$3^+ \rightarrow 4^+$	82-98%M1	2-18%E2	0.0064-0.0065	0.0037±0.0007		
			0-12%M1	88-100%E2	0.0044-0.0069		*	
737.5	+0.282±0.004	$1^- \rightarrow 2^+$	1-86%E1	14-99%M2	0.0040-0.018	0.0020±0.0003		
		$2^- \rightarrow 2^+$	5-63%E1	37-95%M2	0.0079-0.018			
		$3^- \rightarrow 2^+$	99-100%E1	0-1%M2	0.0016-0.0018		*	
			4-9%E1	91-96%M2	0.017-0.018			
748.8	+0.43 ±0.08	$2^+ \rightarrow 3^-$	1-92%E1	8-99%M2	0.0028-0.017	0.0019±0.0002		Anisotropy of a $3^+ \rightarrow 3^-$ E1 transition is negative
		$4^+ \rightarrow 3^-$	93-100%E1	0-7%M2	0.0016-0.0027		*	
			4-12%E1	88-96%M2	0.016-0.017			
831.6	-0.20 ±0.10	$1^- \rightarrow 2^+$	29-93%E1	7-71%M2	0.0022-0.010	0.0022±0.0006	*	
		$2^+ \rightarrow 2^+$	95-100%M1	0-5%E2	0.0049-0.0051			
			4-34%M1	66-96%E2	0.0032-0.0038		*	
859.7	-0.03 ±0.04	$2^+ \rightarrow 2^+$	87-96%M1	4-13%E2	0.0045-0.0046	0.0040±0.0007	*	
			0-12%M1	88-100%E2	0.0029-0.0031		*	
869.3	-0.09 ±0.05	$4^+ \rightarrow 4^+$	80-93%M1	7-20%E2	0.0041-0.0044	0.0054±0.0009	*	
			8-22%M1	78-92%E2	0.0028-0.0031		(*)	
938.2	-0.52 ±0.16							Has not been placed in decay scheme
1046.4 1049.2 }	-0.26 ±0.02							
1166.8	+0.08 ±0.08	$1^- \rightarrow 0^+$	100%E1		0.0007	0.0011±0.0003	*	
1171.1	-0.175±0.013	$3^+ \rightarrow 2^+$	88-93%M1	7-12%E2	0.0022-0.0023	0.0023±0.0006	*	Anisotropy of a $5^+ \rightarrow 2^+$ M3 transition is -0.36
			0-2%M1	98-100%E2	0.0015		*	

Table 5. VII (continued)

E_γ in keV	anisotropy $W(0^\circ)-1$	transition	multipole admixture		range of K-conversion coefficient	experimental K-conversion coefficient	remarks
1178.5	+0.01 ±0.08	$3^- \rightarrow 4^+$	96-100%E1	0-4%M2	0.00068-0.00087	0.00083±0.00027*	
			1-10%E1	90-99%M2	0.0049-0.0054		
		$4^- \rightarrow 4^+$	62-85%E1	15-38%M2	0.0014-0.0025	(*)	
			1-15%E1	85-99%M2	0.0047-0.0054		
		$5^- \rightarrow 4^+$	95-98%E1	2-5%M2	0.00077-0.00092	*	
			0-1%E1	99-100%M2	0.0044		
1194.8	-0.40 ±0.08	$2^+ \rightarrow 0^+$	100%E2		0.0015	0.0015±0.0003	
1248.1	-0.33 ±0.15	$4^+ \rightarrow 4^+$	18-100%M1	0-82%E2	0.0013-0.0017	0.0018±0.0004 *	
1262.4	+0.35 ±0.10						Has not been placed in decay scheme
1309.5	-0.41 ±0.14	$4^+ \rightarrow 2^+$	84-100%E2	0-16%M3	0.0012-0.0022	0.0016±0.0003 *	
			0-16%E2	84-100%M3	0.0064-0.0074		
1323.7	+0.30 ±0.12						Has not been placed in decay scheme
1346.4	+0.39 ±0.04	$5^- \rightarrow 4^+$	96-100%E1	0-4%M2	0.00052-0.00064	0.00053±0.00008*	
			2-9%E1	91-98%M2	0.0033-0.0035	(*)	
		$3^- \rightarrow 4^+$	83-98%E1	2-17%M2	0.00058-0.0010	*	Anisotropy of a $4^- \rightarrow 4^+$ E1 transition is negative
			0-9%E1	81-100%M2	0.0030-0.0036	(*)	

c. Orientation parameters of the capturing state and the 334 and 773 keV levels.

The orientation parameters of the capturing state can be obtained from the anisotropy of the 7212.0 keV transition. If it is assumed that it is a pure $4^- \rightarrow 4^+$ E1 transition the anisotropy $W(0^\circ) - 1 = -1.2\, f_2$, where f_2 is the alignment parameter of the capturing state of ^{150}Sm. From the experimental results it follows that $f_2 = 0.45 \pm 0.04$ for sample I ($W(0^\circ)-1 = -0.54 \pm 0.05$) and $f_2 = 0.29 \pm 0.01$ for sample II ($W(0^\circ)-1 = -0.35 \pm 0.01$). The f_4 parameter of the capturing state can be obtained from the curves in fig. 5.1. The results are $f_4 = 0.037 \pm 0.010$ for sample I and $f_4 = 0.012 \pm 0.003$ for sample II. It should be noted that in order to get the orientation parameters of the ^{149}Sm nuclei these parameters have to be divided by G_2^n and G_4^n. The average temperature of the ^{149}Sm nuclei during the experiments can also be obtained from fig. 5.1. For sample I the average temperature after demagnetization was between 0.006 and 0.014 K; for sample II it was between 0.016 and 0.024 K. The influence of a possible $3^- \rightarrow 4^+$ admixture has been neglected. The orientation parameters obtained would be slightly larger and the average temperature somewhat lower if it had been present. The anisotropy of the 7212.0 keV transition directly after demagnetization was estimated to be -0.58 ± 0.05 (sample I). Assuming that initially the nuclei are completely aligned it can be estimated that the intensity of capture gamma rays from the 3^- bound state to the 4^+ level is less than 19 % of the total intensity of the 7212.0 keV transition.

The orientation parameters of the levels at 334 and 773 keV were also determined experimentally. For this purpose the anisotropy of the directional distribution of the 334 and 440 keV transitions was measured in the $\theta = 0^\circ$ as well as the $\theta = 90^\circ$ direction. Both are pure quadrupole transitions with known spins of the initial and final states. For the $2^+ \rightarrow 0^+$ transition of 334 keV the anisotropies are related to the orientation parameters as follows:

$$W(0^\circ) - 1 = -\frac{10}{7} f_2 - \frac{40}{3} f_4 = -0.298 \pm 0.005,$$

$$W(90^\circ) - 1 = +\frac{5}{7} f_2 - \frac{15}{3} f_4 = +0.129 \pm 0.002.$$

The above-mentioned experimental values were obtained for sample I. Consequently $f_2 = 0.193 \pm 0.002$ and $f_4 = 0.0017 \pm 0.0003$ for the 334 keV

level. In the same way we get for the $4^+ \rightarrow 2^+$ transition of 440 keV:

$$W(0^\circ) - 1 = -\frac{60}{49} f_2 - \frac{64}{21} f_4 = -0.393 \pm 0.005,$$

$$W(90^\circ) - 1 = +\frac{30}{49} f_2 - \frac{24}{21} f_4 = +0.166 \pm 0.003,$$

again for sample I. We obtain $f_2 = 0.292 \pm 0.003$ and $f_4 = 0.011 \pm 0.002$ for the 773 keV level. By comparing the anisotropies of the 334 and 440 keV transitions of the samples I and II the f_2 and f_4 parameters of the 334 and 773 keV levels (in sample II) could be estimated. For example, the parameters obtained in this way for the 773 keV level are: $f_2 = 0.200 \pm 0.005$ and $f_4 = 0.008 \pm 0.002$.

d. Neutron-capture gamma-ray spectra at 0.047 and 0.125 eV neutron energy.

Some experiments were performed in which the neutron-capture gamma-ray spectra above 5 MeV were compared for neutron energies of 0.047 and 0.125 eV. After normalizing to the strongest transition of 7212.0 keV and subtracting the two spectra only background peaks were left and no evidence could be found for a difference in intensity of the samarium peaks. At the neutron energy of 0.125 eV, neutron capture in the bound state as compared to capture in the resonance at 0.0976 eV will be about 1.6 times less than at 0.047 eV. Although the statistical errors were rather large the experiment showed that there is no transition with an intensity greater than 0.03 gamma's per 100 neutrons captured which mainly proceeds from the bound state to some discrete low energy level of ^{150}Sm.

5. Analysis of results

a. Anisotropy of the high energy transitions of ^{150}Sm.

In the analysis of the results we assume that the observed high energy transitions are pure dipole transitions. In addition it is assumed that they proceed from the capturing state which is justified by the the same arguments as used in section 4.6.a. The multipolarity and electromagnetic character of the primary transitions can to some extent be predicted if the electron conversion coefficients are known. The electron conversion spectrum of ^{150}Sm at low as well as at high energies has been measured by Elze[3]. In order

to get an interpretation of his results Elze extrapolated the theoretical curves of the conversion coefficients by drawing tangents to these curves plotted on a double logarithmic scale since above 2.6 MeV the coefficients had not been calculated. The result was that the expected M1 and E1 coefficients are equal at 9 MeV. However, there is now some evidence both experimental and theoretical that it is not correct to extrapolate in this way. According to Smither[40] the ratio between the measured values of conversion coefficients of M1 and E1 transitions at 9 MeV is 1.7 for ^{114}Cd, although nearly equal conversion coefficients are expected if theoretical curves, extrapolated in the same way as done by Elze, are used. In addition calculations of high energy K-shell conversion coefficients have been performed for this nucleus by Church and Wesener[41]. They also find that M1 and E1 conversion coefficients are different at 9 MeV although their ratio is only 1.2. The same kind of calculation performed for samarium[42] shows that in the energy region of interest (5.3 - 7.2 MeV) the ratio between electron conversion coefficients of M1 and E1 transitions is about 1.4. Therefore it seemed worth while to reanalyse the conversion data of Elze. The conversion coefficients were calculated using the electron intensities of ref. 3 and the gamma intensities of ref. 2 and table 5.IV. It is assumed that the 7212.0 keV transition has E1 character. Its conversion coefficient was used to extrapolate the theoretical curve above 2.6 MeV. The relation between E1 and M1 conversion coefficients and the energy of the gamma rays, plotted on a double logarithmic scale, can be approximated by a straight line in the energy interval between 5.3 and 7.2 MeV. The expected experimental conversion coefficients for M1 transitions were derived from the ratio between the calculated E1 and M1 coefficients given in ref. 42. The tentative multipole assignments derived from the conversion coefficients are given in column 4 of table 5.VI. The occurrence of quadrupole transitions has not been considered since they seem to be less probable. For some transitions no conversion electrons have been observed although the electron intensity should be sufficient according to the gamma intensities given by Groshev[2]. These transitions were assumed to have E1 character if the intensity is greater than or equal to 0.02 gamma's per 100 neutrons captured. They are indicated with an asterisk in table 5.VI.

Taking into account the results of section 5.4.d it is assumed that the influence of the negative resonance with spin 3 is negligible for gamma transitions with intensities greater than 0.03 gamma's per 100 neutrons captured

and thus that for the interpretation of the anisotropy measurements the spin of the capturing state can be assumed to be 4. For gamma transitions with an intensity less than 0.03 gamma's per 100 neutrons captured the possibility that there is an appreciable contribution of capture in the negative resonance with spin 3 has not been neglected.

The expected anisotropies of high energy transitions, assuming dipole character, can be calculated. The results for the three possible spin values of the final state are:

$$4 \rightarrow 5 \qquad W(0^{o})-1 = +\frac{24}{55} f_2 G_2^n,$$

$$4 \rightarrow 4 \qquad W(0^{o})-1 = -\frac{6}{5} f_2 G_2^n,$$

$$4 \rightarrow 3 \qquad W(0^{o})-1 = +\frac{6}{7} f_2 G_2^n.$$

It is assumed that the 7212.0 keV transition is a $4^{-} \rightarrow 4^{+}$ E1 transition. Its measured anisotropy is $W(0^{o})-1 = -0.35 \pm 0.01$ (sample II). Consequently the expected anisotropies for $4 \rightarrow 5$ and $4 \rightarrow 3$ transitions are +0.13 and +0.25 respectively. The spin values of the final levels which can be concluded from the anisotropy measurements on the basis of the anisotropies of pure dipole transitions are given in column 6 of table 5.VI. The parities are derived from the characteristics of the primary transitions given in column 4 of table 5.VI.

The anisotropy of the directional distribution is very sensitive to quadrupole admixture. The limits of the possible quadrupole admixtures in the high energy gamma rays are given in column 7 of table 5.VI. For all levels with assigned spin 4 the quadrupole admixture in the corresponding high energy gamma rays is greater than 30 % if a spin 3 or 5 is assumed instead. In the same way high energy gamma rays corresponding to levels assigned with spin 3 or 5 have a quadrupole admixture greater than 9 % if spin 4 is assumed. Therefore these possibilities are rejected.

b. Anisotropy of the low energy transitions of ^{150}Sm.

The disorientation parameters G_k in formula 2.2, which depend on the spins of the final states, were calculated using the two models outlined in chapter II. The parameters used for the Monte-Carlo programme are: $\sigma = 5$, $a = 22.0$ MeV^{-1}, $\Delta = 1.25$ MeV, $J = I + \frac{1}{2} = 4$, and the pseudo continuum was thought to extend above 2.4 MeV. Weisskopf estimates were

used for the relative probabilities of the different dipole and quadrupole transitions. The results for the G_k parameters can be found in table 5.VIII.

Table 5.VIII.

Calculated values of the disorientation parameters G_2 and G_4 for ^{150}Sm.

spin of final level	Monte Carlo programme		simplified programme with ν is 3.	
	G_2	G_4	G_2	G_4
1^-	0.24 ± 0.05			
1^+	0.33 ± 0.07		0.53	
2^-	0.55 ± 0.05	0.06 ± 0.06		
2^+	0.52 ± 0.05	0.01 ± 0.01	0.56	0.00
3^-	0.60 ± 0.05	0.12 ± 0.01		
3^+	0.65 ± 0.06	0.18 ± 0.02	0.64	0.16
4^-	0.64 ± 0.05	0.21 ± 0.02		
4^+	0.65 ± 0.06	0.22 ± 0.02	0.66	0.21
5^-	0.64 ± 0.03	0.23 ± 0.01		
5^+	0.65 ± 0.09	0.26 ± 0.04	0.70	0.32
6^+	0.68 ± 0.07	0.32 ± 0.03	0.71	0.41

The average number of transitions from the capturing state to the ground state was calculated to be 6.0 which compares very well to the experimental value 6.3 ± 0.3 obtained by the authors of ref. 43. This means that the average number of transitions between the capturing state and energy levels which mainly decay to the lowest 4^+ and 2^+ levels is about 3 to 4. The disorientation parameters were also calculated with the more simple model in which the number of transitions, ν, from the capturing state to some energy level is kept fixed. Table 5.VIII shows that there is a rather good correspondence between the G_k parameters obtained with the two models for $\nu = 3$ except for levels with spin 1. From the experimentally determined orientation parameters of the 4^+ level at 773 keV and the capturing state it is possible to derive the disorientation parameters for the 773 keV level. The result is: $G_2 = 0.72 \pm 0.03$ and $G_4 = 0.35 \pm 0.14$ which is in reasonable agreement with the predicted values in table 5.VIII for a 4^+ state.

For several combinations of spins of the initial and final states

the expected anisotropies were calculated as a function of the mixing parameter using the G_k values of table 5.VIII and the parameters f_2 and f_4 of the capturing state given in section 5.4.c. Terms with k greater than 4 were omitted since they are negligibly small. The results for mixed dipole-quadrupole transitions with initial spin 4 are given in fig. 5.10 and compared

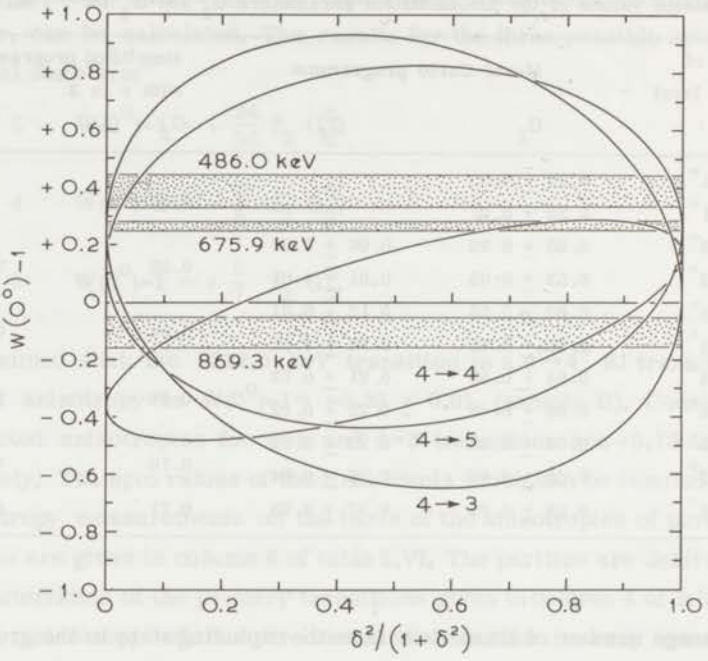

Fig. 5.10. Expected anisotropies of some low energy transitions in ^{150}Sm as a function of $\delta^2/(1+\delta^2)$.

to some of the measured anisotropies. The errors given in table 5.VIII include statistical errors and the variation of G_k with the excitation energy. Additional errors may occur due to the simplifying assumptions which were made. It is assumed that the total errors in the G_2 parameters is less than 15 % if the spin of the final level is 2 or more. The errors in the G_4 parameters are larger but their influence on the analysis is rather small.

The conclusions which can be drawn from the anisotropy measurements can be found in table 5.VII. In addition to the anisotropies the expected electron conversion coefficients are given together with the experimental conversion coefficients. The spin values consistent with the anisotropy and conversion data are indicated by an asterisk.

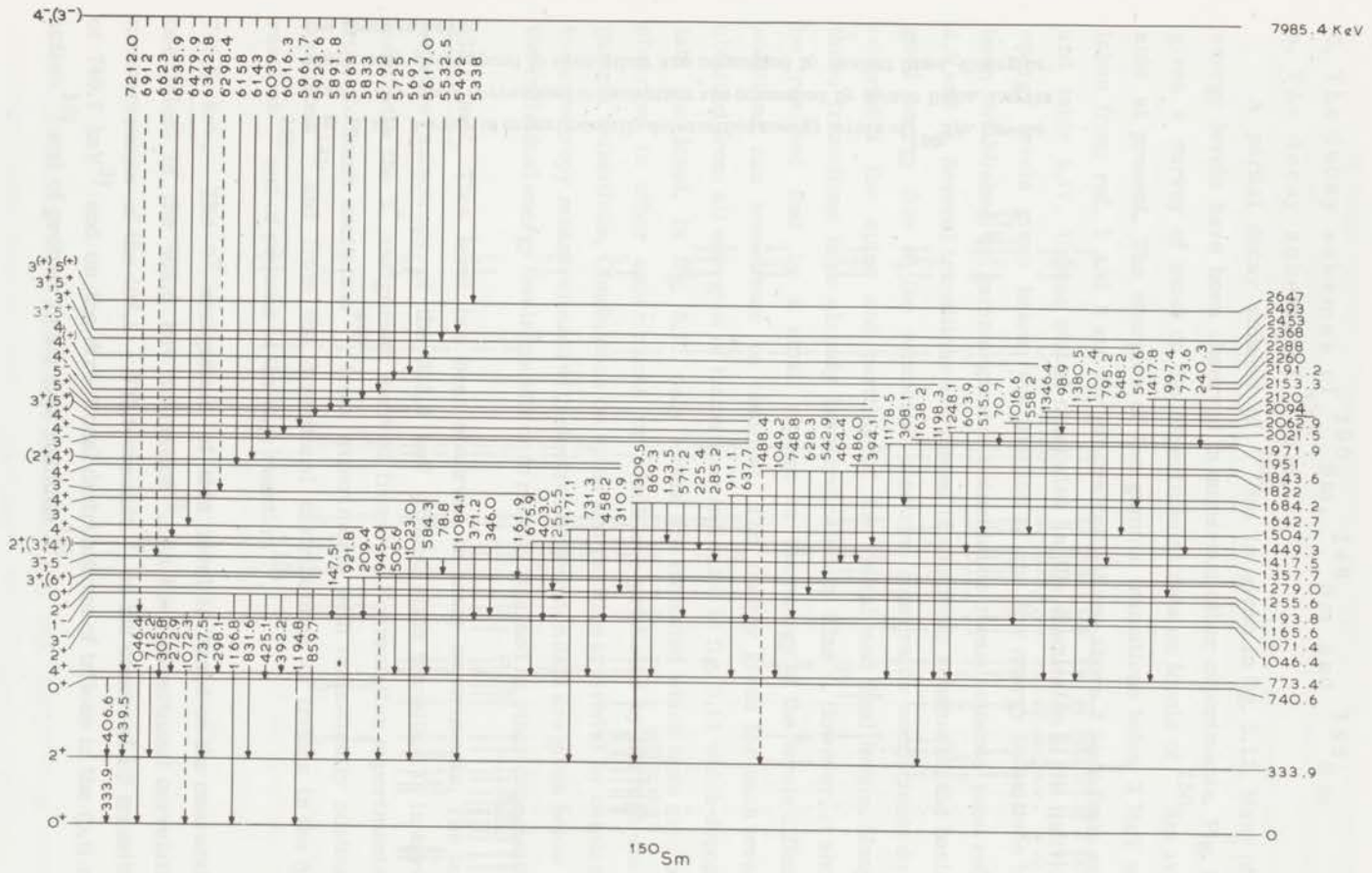

Fig. 5.11. Decay scheme of ^{150}Sm. Energies in keV.

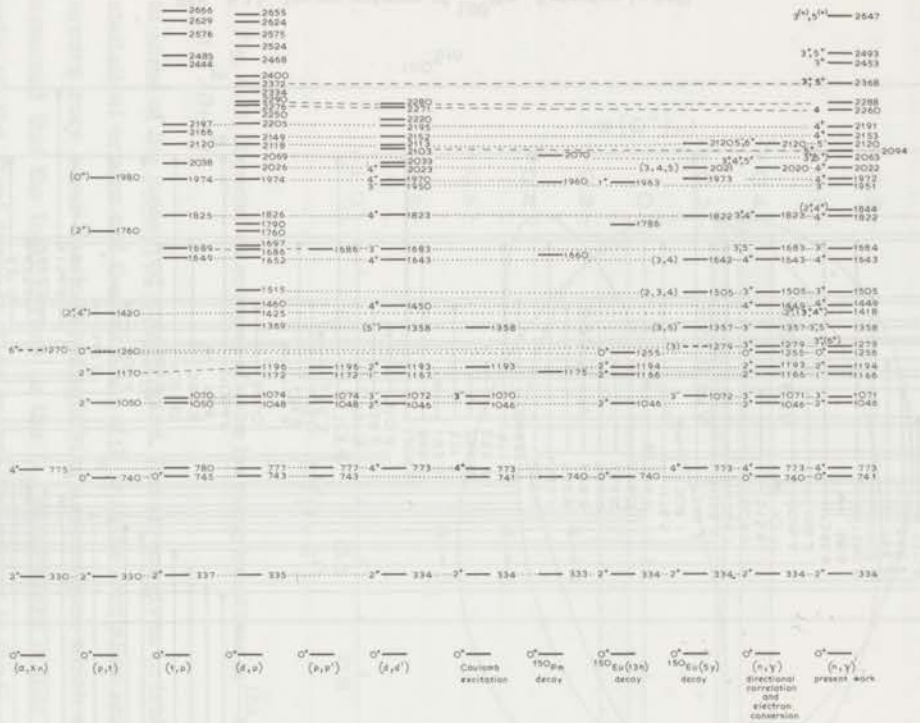

Fig. 5.12. Survey of experimentally determined energy levels of ^{150}Sm. Levels which very likely correspond to each other are connected by dotted lines. Levels which may correspond to each other are connected by dashed lines. Energies are given in keV.

6. The decay schemes of ^{150}Sm, ^{148}Sm and ^{153}Sm

a. The decay scheme of ^{150}Sm.

A partial decay scheme of ^{150}Sm is given in fig. 5.11. Many of the energy levels have been observed in numerous other experiments. Fig. 5.12 gives a survey of most of the experimental data on levels of ^{150}Sm available at present. The energies of the gamma transitions below 3 MeV were taken from ref. 1 and 3 and for gamma transitions above 3 MeV from ref. 2 and table 5.IV. Unless stated otherwise in the discussion of the individual energy levels given below, the position of the low energy transitions have been established by gamma-gamma coincidence measurements (see ref. 1, 4,5 and 7). Several transitions are placed in the decay scheme on the basis of good energy fits if the measured electron conversion coefficients do not contradict the spins and parities of the initial and final levels. Many of these transitions have already been indicated by Elze[3]. However, it should be realised that by a small change in the energy of the levels different solutions can sometimes be obtained. The energy given for each level is obtained from all energies of transitions indicated in fig. 5.11 which depopulate the level. In fig. 5.11 only levels are indicated which have also been observed in other experiments or which are predicted by the high energy gamma transitions. Conclusions on spins and parities arrived at by combining the anisotropy measurements with electron conversion data are given below for the individual energy levels in addition to results obtained in other experiments.

333.9 keV. This level has been observed in many experiments. The large negative anisotropy of the 333.9 keV ground state transition is in agreement with the 2^+ assignment derived from $\gamma - \gamma$ correlation experiments[7], from Coulomb excitation[44], from experiments with inelastically scattered deuterons[12] and from the directional distributions of tritons in the (p,t) reaction[16] and of protons in the (t,p) reaction[15].

740.6 keV. The 0^+ assignment of this level is based on the conversion coefficient of the 406.6 keV transition[3], on $\gamma - \gamma$ directional correlation measurements of the 406.6 - 333,9 cascade[7], on the observed E0 transition of 740.7 keV[3] and on the directional distributions of tritons in the (p,t) reaction[16] and of protons in the (t,p) reaction[15].

773.4 keV. the 4^+ assignment of this level is firmly established by $\gamma-\gamma$ directional correlation experiments [1,7] and by experiments with inelastically scattered deuterons[12] and heavy ions [44]. The 439.5 keV transition showed a large negative anisotropy in agreement with a $4^+ \rightarrow 2^+$ E2 transition.

1046.4 KeV. The anisotropy and electron conversion coefficient of the 712.2 keV transition restrict the spin of this level to $1^\pm$, $2^\pm$ or 3^+. The 1046.4 keV ground state transition has a conversion coefficient which is too small for a $3^+ \rightarrow 0^+$ transition. Therefore a spin and parity 3^+ can be rejected for the 1046.4 keV level. The 403.0 keV transition has been placed between the 1449.3 keV level, which will be shown to be a 4^+ level, and the level at 1046.4 keV[1]. The large negative anisotropy of the 403.0 keV transition and its conversion coefficient further restrict the spin and parity of the 1046.4 keV level to 2^+. The 1046.4 keV transition to the ground state could not be separated from the 1049.2 keV transition. The negative anisotropy of the composite peak must be partly due to the $2^+ \rightarrow 0^+$ ground state transition. The 272.9 and 305.8 keV transitions, of which the latter has also been observed in the decay of ^{150}Eu (13 h), fit very well between the 1046.4 keV state and the levels at 773.4 keV and 740.6 keV, respectively. A 2^+ assignment for the 1046.4 keV level has also been derived from $\gamma-\gamma$ correlation experiments[1], from the directional distribution of inelastically scattered deuterons[12] and from the directional distribution of tritons in the (p,t) reaction[16].

1071.4 keV. The only possible assignment compatible with the anisotropy of the 737.5 keV transition and its conversion coefficient is 3^-. A transition of 298.1 keV from this state to the level at 773.4 keV has also been observed in the decay of ^{150}Eu (5 y) [7]. A weak transition of 1072.3 keV has been reported by Elze[3] which might be the cross-over to the ground state. A very weak high energy transition of 6912 keV possibly proceeds from the capturing state to this level. A 3^- assignment has also been derived from the directional correlation between scattered heavy ions and gamma rays after Coulomb excitation[44], from $\gamma-\gamma$ correlation experiments[1] and from the directional distribution of inelastically scattered deuterons[12].

1165.6 keV. This level was previously assigned as 2^+ on the basis of the directional correlation of the 831.6 and 333.9 keV transitions[7]. However,

the directional distribution of inelastically scattered deuterons favours a 1^- assignment[12]. In addition the anisotropy of the 1166.8 ± 1.0 keV ground state transition, which is assumed to be identical with the 1165.7 keV transition observed in the decay of ^{150}Eu (13 h)[8], does not have the large negative value expected for a $2^+ \rightarrow 0^+$ transition. The only possibility which is in agreement with the experimental data is a $1^- \rightarrow 0^+$ transition. The 831.6 keV transition is a mixed E1-M2 transition. The 425.1 and 392.2 keV transitions, the first of which has also been observed in the decay of ^{150}Eu (13 h) [8], fit very well between the 1165.6 keV level and the 740.6 and 773.4 keV levels.

1193.8 keV. The spin of this level is restricted to 2^+ by the large negative anisotropy of the 1194.8 ± 0.9 keV transition to the ground state. The 859.7 keV $2^+ \rightarrow 2^+$ transition is a mixed M1-E2 transition. The 147.5 keV transition is tentatively placed in the decay scheme between the levels at 1193.8 and 1046.4 keV since the energy fit is very good. A 2^+ assignment for the 1193.8 keV level has also been obtained by the authors of ref. 12.

1255.6 keV. This level has been observed in the decay of ^{150}Eu (13 h)[7,8]. The directional correlation of the 921.8 and 333.9 keV gamma's is only in agreement with a 0-2-0 sequence[7]. In addition E0 transitions of 514.7 and 1256.3 keV have been observed by Elze[3]. These lines fit between the 1255.6 keV level, the 0^+ state at 740.6 keV and the ground state, respectively. A 0^+ assignment has also been derived from the directional distribution of tritons in the (p,t) reaction[16]. The 209,4 keV transition has also been observed in the decay of ^{150}Eu (13 h) between the 1255.6 keV level and the level at 1046.4 keV.

1279.0 keV. The large negative anisotropy of the 505.6 keV transition and its conversion coefficient restrict the spin and parity of this level to $3^\pm$, $4^\pm$, $5^\pm$ or 6^+. In all cases, except for the $6^+ \rightarrow 4^+$ transition, quadrupole-dipole mixtures must be assumed. The $\gamma - \gamma$ directional correlation experiments of Smither[1] are only in agreement with a 2^+ or 3^+ assignment for the 1279.0 keV level. In this case also mixed transitions are necessary to understand the observed correlations. Experiments with the (α,xn) reaction[13] suggest however that there is a 6^+ level at 1279 keV in ^{150}Sm. Hence the information obtained hitherto is rather contradictory if a single level at 1279 keV is assumed. Most of the information points to a 3^+ assignment but 6^+ cannot be fully rejected. In both cases the 505.6 keV transition is a comparatively

strong transition to the 4^+ level at 773.4 keV which is generally assumed to be a 'two-phonon state'. Consequently the 1279.0 keV level might be a 'three-phonon state'. If it is a 3^+ state a transition to the 2^+ 'two-phonon state' is expected but has not been observed. In addition the level should have been observed in Coulomb excitation or in the (d,d') reaction. If the 6^+ assignment is accepted, the 945.0 keV transition has been wrongly placed between the levels at 1279.0 and 333.9 keV. Finally a 6^+ assignment fits very well in the systematics of levels of neighbouring even-even nuclei (see chapter VI).

1357.7 keV. The anisotropy and conversion coefficient of the 584.3 keV transition restrict the spin and parity of this level to 3^- or 5^- (see table 5.VII). The same restriction can be deduced from the γ-γ correlation experiments of Smither[1]. He suggested an assignment 3^- since there are two gamma transitions, of 1023.0 and 78.8 keV, which might connect the 1357.7 keV level with a 2^+ and a 3^+ state. The same spin assignment has been obtained from γ-γ correlation experiments on the 1023.0 - 333.9 cascade[4]. Experiments with inelastically scattered deuterons suggested however, that the 1357.7 keV level is a 5^- level. The high energy gamma transition of 6623 keV may proceed to the 1357.7 keV level.

1417.5 keV. A level at about this energy has been observed in the (d,p) and (p,t) reactions [14,16]. The γ-γ coincidence measurements of Smither[1] suggest that the 346.0 and 1084.1 keV transitions proceed from this level to the 3^- level at 1071.4 keV and the 2^+ level at 333.9 keV.
Since the 346.0 keV transition has E1 character the spin is restricted to 2^+, 3^+ or 4^+. The directional distribution of tritons in the (p,t) reaction[16] is in agreement with a 2^+ or 4^+ assignment for this level. The gamma transitions of 161.9 and 371.2 keV also fit between this level and the levels at 1255.6 and 1046.4 keV. If the 161.9 keV transition is placed correctly its conversion coefficient further restricts the spin and parity of the 1417.5 keV level to 2^+.

1449.3 keV. The spin and parity of this level are restricted to 4^+ by the anisotropy and conversion coefficient of the 6535.9 keV transition. The 675.9 keV transition, of which an anisotropy has been measured, is an E0-M1-E2 transition with at least 0.3 % E0 admixture. The 255.5 keV transition is placed in the decay scheme between the 1449.3 keV level an the level at 1193.8 keV. A 4^+ assignment for the 1449.3 keV level has also been obtained by the authors of ref. 1 and 12.

1504.7 keV. The spin and parity of this level are restricted to 3^+ or 5^+ by the anisotropy and the conversion coefficient of the 6479.9 keV transition. The 5^+ value is rejected since the conversion coefficient of the 1171.1 keV transition is too small for a $5^+ \rightarrow 2^+$ (M3) transition. The anisotropy of the 1171.1 keV transition corresponds however very well with a $3^+ \rightarrow 2^+$ dipole or quadrupole transition. The anisotropy of the 731.3 keV transition is in agreement with a $3^+ \rightarrow 4^+$ E2 transition. The 458.2 and 310.9 keV transitions also fit very well in the decay scheme between the 1504.7 keV level and the levels at 1046.4 and 1193.8 keV. A spin and parity 3^+ have also been obtained by Smither[1].

1642.7 keV. The spin of this level is 4^+ which can be concluded directly from the anisotropy and the conversion coefficient of the 6342.8 keV transition. The 1309.5 and 869.3 keV transitions have also been observed in the decay of ^{150}Eu (5 y)[7]. The large negative anisotropy of the 1309.5 keV transition is in agreement with a $4^+ \rightarrow 2^+$ E2 transition. The 869.3 keV transition is possibly a mixed E0-M1-E2 transition. The 571.2 keV transition has been placed between the 1642.7 keV level and the 3^- level at 1071.4 keV[1]. The anisotropy and electron conversion coefficient of this transition are in agreement with a $4^+ \rightarrow 3^-$ E1 transition. A 4^+ assignment has also been derived from γ-γ correlation experiments[1] and from the directional distribution of inelastically scattered deuterons[12]. In addition transitions of 193.5, 225.4 and 285.2 keV are placed in the decay scheme between the 1642.7 keV level and the levels at 1449.3, 1417.5 and 1357.7 keV.

1684.2 keV. The 911.1 keV transition has been proved to be coincident with the 439.5 keV transition[4]. Consequently a level at about 1684 keV can be expected. The 637.7 keV transition fits well between the 1684.2 keV level and the level at 1046.4 keV. The conversion coefficients of these two transitions restrict the spin and parity of the 1684.2 keV level to 3^- or 4^- while the γ-γ correlation measurements of ref. 4 give a restriction to 5^- or 3^-. Consequently the spin of the 1684.2 keV level very likely is 3^- and corresponds to the level at 1683 keV with the same spin and parity which has been observed in experiments with inelastically scattered deuterons[12]. It is not certain that the 6298.4 keV transition, which has a negative anisotropy, proceeds to the level at 1684.2 keV. If it does, the 6298 keV transition might be a $3^- \rightarrow 3^-$ transition (see table 5.VI).

1822 keV. This level has been observed in several particle reactions. The gamma transitions of 464.4, 748.8, 1049.2 and 1488.4 keV, which are placed between this level and levels with a lower energy, have also been observed in the decay of ^{150}Eu (5 y)[7]. The anisotropy and the conversion coefficient of the 748.8 keV transition are only in agreement with a 4^+ assignment for this level. Directional correlation measurements on the 748.8 - 737.5 cascade [4,7] are in agreement with a spin 3 or 4. A 4^+ assignment is also in agreement with the directional distribution of inelastically scattered deuterons[12]. The primary gamma ray of 6158 keV probably proceeds to the 1822 keV level. It shows a negative anisotropy, in agreement with a $4^- \rightarrow 4^+$ dipole transition. In addition to the gamma rays mentioned above the 628.3 and 542.9 keV transitions are also fitted in the decay scheme between the 1822 keV level and the levels at 1193.8 and 1279.0 keV.

1843.6 keV. On the basis of the high energy transition of 6143 keV a level at about 1843 keV is predicted. By looking for gamma transitions which might proceed from this level to levels of lower energy the best energy fit was obtained for the two transitions of 394.1 and 486.0 keV. Assuming that the 486.0 keV transition is placed correctly the spin and parity of the 1843.6 keV level are restricted to 2^+, 4^+ or 6^+. (See table 5.VII.). Since the 6143 keV transition is likely to be a dipole transition 6^+ can be excluded. The intensity of the 6143 keV transition is very low therefore not much information can be obtained from the anisotropy of this transition.

1951 keV. On the basis of the high energy gamma transition of 6039 keV a level at about 1950 keV is predicted. It has been shown by Zehender and Fleischmann[5] that there is a transition from this level to the 773.4 keV state. The 1178.5 keV (1176.6) transition observed by the authors of ref. 1 and 3 is the only one which can be placed between the 1951 and 773.4 keV levels. The anisotropy an the conversion coefficient of this transition restrict the spin and parity of the 1951 keV level to 3^-, 5^- or (4^-). The proposed M1 character of the 6039 keV primary transition is in agreement with this assignment. The 308.1 keV transition fits well between the 1951 keV level and the level at 1642.7 keV. The 1951 keV level corresponds very likely to the level at 1950 keV observed in the (d,d') reaction[12], where the directional distribution is in agreement with that of a 3^- level.

1971.9 keV. It has been shown that there is a two-step cascade from the capturing state to the 2^+ level at 333.9 keV and possibly another one to the 4^+ level at 773.4 keV in which this level is the intermediate state[5]. The transitions to the 2^+ and 4^+ levels are very likely the 1638.2 and 1198.3 keV transitions which have also been observed in the decay of ^{150}Eu (5 y)[7]. The anisotropy of the 6016.3 keV transition restricts the spin of the 1971.9 keV level to 4. It very likely corresponds to the levels which have been observed at about 1970 keV in the (d,p), (t,p) and (d,d') reactions [14,16,12]. A spin and parity 4^+ have been assigned by the authors of ref. 12.

2021.5 keV. This level has been observed in the decay of ^{150}Eu (5 y)[7] and decays with a 1248.1 keV transition to the 773.4 keV state. The anisotropy and conversion coefficient of the 5961.7 keV transition show that the 2021.5 keV level is a 4^+ level. The anisotropy of the 1248.1 keV transition is in agreement with a $4^+ \rightarrow 4^+$ transition. The 515.6 keV transition between the levels at 2021.5 and 1504.7 keV has also been found in the decay of ^{150}Eu (5 y)[7]. The 70.7 keV transition is tentatively placed between the levels at 2021.5 and 1951 keV. The 2021.5 keV level has also been observed in the (d,p) and (d,d') reactions [14,12]. The 4^+ assignment is in agreement with the results obtained with the (d,d') reaction[12].

2062.9 keV. The high energy gamma transition of 5923.6 keV shows a positive anisotropy which restricts the spin of the 2062.9 keV level to 3^+ or 5^+ (see table 5.VI). The 558.2 and 1016.6 keV transitions are tentatively placed in the decay scheme between this level and the levels at 1504.7 and 1046.4 keV. The anisotropy of the 558.2 keV transition is in agreement with a $3^+ \rightarrow 3^+$ transition and excludes a 5^+ assignment. The 2062.8 keV level may correspond to the level at 2069 keV observed in the (d,p) reaction [14].

2094 keV. This level is predicted by the high energy transition of 5891.8 keV. It may correspond to the level at 2103 keV observed in the (d,p) reaction [14]. A 5^+ assignment is concluded from the anisotropy of the 5891.8 keV transition (see table 5.VI).

2120 keV. This level has been observed in the decay of ^{150}Eu (5 y) [7] and very likely in the (d,p) and (t,p) reactions [14,16]. The 1346.4 keV transition to the level at 773.4 keV, which has also been observed in the decay mentioned

above, showed a large positive anisotropy. This anisotropy together with the conversion coefficient restrict the spin of the 2120 keV level to 3^- or 5^-. The 5^- assigment is in agreement with the γ-γ correlation experiments of ref. 4. By looking for other transitions which also fit in the decay scheme only the 98.9 keV transition was found which is tentatively placed between the levels at 2120 and 2021.5 keV. The 5863 keV transition observed by Groshev [1] may proceed to the 2120 keV level.

2153.3 keV. This state corresponds to energy levels which have been found in the (d,p), (d,d') and possibly the (t,p) reactions [14,12,16].
On the basis of the anisotropy of the 5833 keV transition this level will be a 4^+ level (see table 5.VI). Transitions with an energy of 1380.5, 1107.4, 795.2, 648.2 and 510.6 keV depopulating this level are put in the decay scheme on the basis of good energy fits.

2191.2 keV. If the 5792 keV transition to this level is a pure dipole transition the spin will be 4 (see table 5.VI). The conversion coefficients of the 1417.8, 997.4, 773.6 and 240.3 keV transitions, which are placed in the decay scheme because of good energy fits, are in agreement with a 4^+ assignment for the 2191.2 keV level. Levels of the same energy have been observed in the (t,p) and (d,d') reactions [16,12].

2260 keV. Assuming that the high energy transition to this level is a pure dipole transition its anisotropy gives a spin 4. This level may also have been observed in the (d,p) and (d,d') reactions.

2368 keV. This level may correspond to the level at 2372 keV observed in the (d,p) reaction [14]. The 3^+ or 5^+ assignment is based on the anisotropy of the 5617 keV transition and its conversion coefficient.

2453 keV. The 3^+ assignment was obtained from the anisotropy measurements (see table 5.VI).

2493 keV. The assignment of this level is 3^+ or 5^+ since the anisotropy of the 5492 keV transition is positive (see table 5.VI).

2647 keV. The assignment of this level is $3^{(+)}$ or $5^{(+)}$ (see table 5.VI).

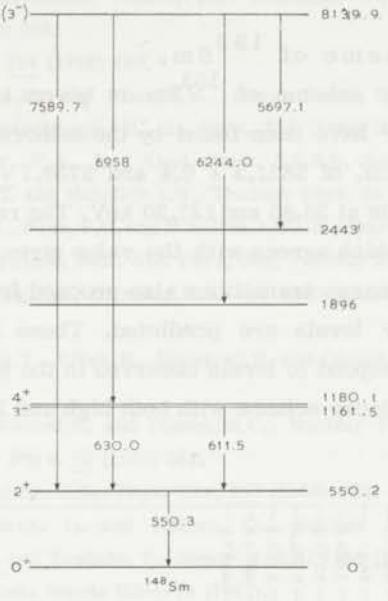

Fig. 5.13. Decay scheme of ^{148}Sm. Energies in keV.

b. The decay scheme of ^{148}Sm.

A partial decay scheme of ^{148}Sm is given in fig. 5.13. The lowest three excited levels at 550.2, 1161.5 and 1180.1 keV and their spins and parities are accepted in accordance with data available from the literature[17]. The gamma transition, of 7589.7 $\pm$ 1.1 keV, is known to proceed to the 2^+ level at 550.2 $\pm$ 0.1 keV. Hence the neutron binding energy is 8139.9 $\pm$ 1.2 keV, in good agreement with the value given in ref. 47 (see table 5.I). The 6958 $\pm$ 2 keV transition fits between the capturing state and the 4^+ level at 1180.1 keV. Assuming that the 6244.0 and 5697.1 keV gamma's are primary

transitions levels at 1896 and 2443 keV are postulated. The 1896 keV level may correspond to a level at 1894.9 keV observed in the decay of ^{148}Eu. No level corresponding to the level at 2443 keV could be found in the literature.

c. The decay scheme of ^{153}Sm.

A partial decay scheme of ^{153}Sm is given in fig. 5.14. The energy levels up to 414 keV have been found by the authors of ref. 21 and 22. The high energy transitions, of 5831.2 ± 0.4 and 5739.7 ± 0.4 keV, are assumed to proceed to the levels at 35.85 and 127.30 keV. The resulting binding energy is 5867.0 ± 0.4 keV, which agrees with the value given in table 5.I. Assuming that the other high energy transitions also proceed from the capturing state several other energy levels are predicted. These levels are indicated in fig. 5.14 if they correspond to levels observed in the (d,p) reaction or if they can be fitted in the decay scheme with both high and low energy transitions.

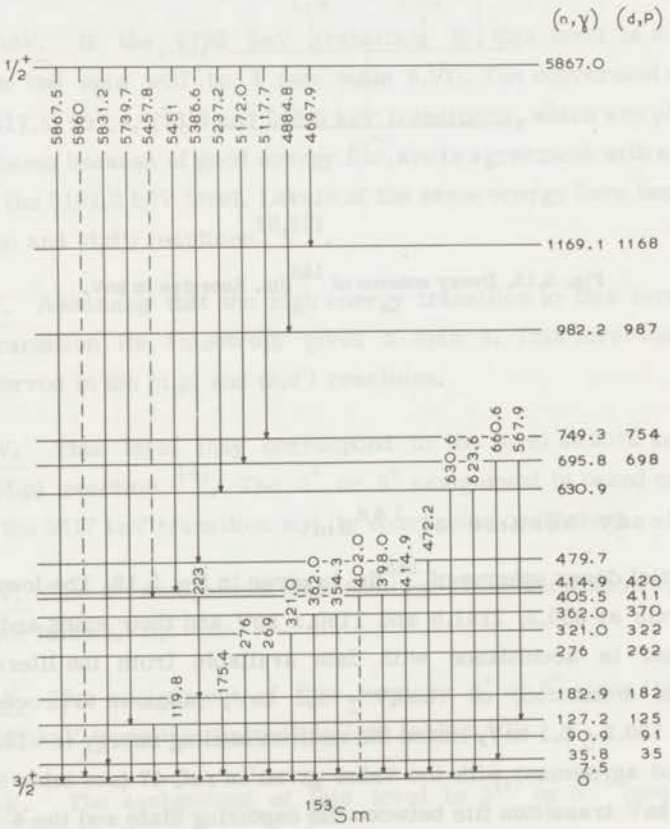

Fig. 5.14. Decay scheme of ^{153}Sm. Energies in keV.

REFERENCES

1. Smither, R.K., Phys. Rev. 150 (1966) 964.
2. Groshev, L.V., Demidov,A.M., Ivanov,V.A., Lutsenko,V.N. and Pelekhov,V.I., Nuclear Phys. 43 (1963) 669.
3. Elze, Th.W., Z. Phys. 194 (1966) 280.
4. Cojocaru, V., Petrascu,M. and Stanciu,M., Revue Roum. Phys. 11 (1966) 283.
5. Zehender, O. and Fleischmann, R., Z. Phys. 183 (1965) 217.
6. Gavor, L.I. and Ivanov, V.A., Izv. Akad. Nauk. S.S.S.R. Ser. Fiz. 31 (1967) 277.
7. Guttman, M., Funk,E.G. and Mihelich,J.W., Nuclear Phys. 64 (1965) 401.
8. Kugel, H.W., Buss.D.J., Funk, E.G. and Mihelich,J.W., Nuclear Phys. 115 (1968) 385.
9. Gove, N.B. and O'Kelly,G.D., Bull. Am. Phys. Soc. 7 (1962) 352.
10. Seaman, G.G., Greenberg,J.S., Bromley,D.A. and McGowan,F.K., Phys. Rev. 149 (1966) 925.
11. Keddy, R.J., Yoshizawa,Y., Elbek,B., Herskind,B. and Olesen,M.C., Nuclear Phys. 113 (1968) 676.
12. Veje, E., Elbek,B., Herskind,B. and Olesen,M.C., Nuclear Phys. 109 (1968) 489.
13. Morinaga, H., Nuclear Phys. 75 (1966) 385.
14. Kenefick, R.A. and Sheline, R.K., Phys. Rev. 133 (1964) B25.
15. Bjerregaard,J.H., Hansen, O. and Nathan, O., Nuclear Phys. 86 (1966) 145.
16. Ishizaki, Y., Sasaki,K. and Yoshida, Y., Report JAERI 1158 (1968) 47.
17. Martin,M.J., Nuclear Data Sheets B2-4-79 (1967).
18. Avotina,M.P., Grigorev,E.P., Zolotavin,A.V., Sergeev,V.O., Sovtsov,M.I., Vrzal,Ya. Lebedev,N.A., Liptak,Ya. and Urbanets,Ya., J.I.N.R. report 3471 (1967).
19. Kenefick,R.A. and Sheline,R.K., Phys. Rev. 139 (1964) B1479.
20. Kotajima,K., Nuclear Phys. 39 (1962) 89.
21. Smither,R.K., Bull. Am. Phys. Soc. 12 (1967) 1065.
22. V.Egidy, T., Mahlein,H.F., Kaiser,W., Dutta,B.C., Jones,A. and Suarez,A.A., Jül. Conf. 1967.
23. Cooke,A.H. and Duffus,H.J., Proc. Roy. Soc. (London) A229 (1955) 407.
24. Judd, B.R., Proc. Roy. Soc. (London) A232 (1955) 458.
25. Marshak, H., Postma,H., Sailor,V.L., Shore,F.J. and Reynolds,C.A., Phys. Rev. 128 (1962) 1287.
26. Hughes,D.J. and Schwartz,R.B., B.N.L. report 325 (1958).
27. Höhne, P., Ann. Physik 7 (1961) 50.
28. Pattenden, N.J., Proc. of the second international conference on the peaceful uses of atomic anergy, Geneva, Vol. 16 (1958) 44.
29. Brockhouse,B.N., Can. J. Phys. 31 (1953) 432.
30. Roberts, L.D., Bernstein,S., Dabbs,J.W.T. and Stanford,C.P., Phys. Rev. 95 (1954) 105.
31. Carpenter,R.T., A.N.L. report 6589 (1962).

32. Poortmans, F. and Ceulemans,H., Intern. Conf. on the study of nuclear structure with neutrons, Antwerpen (1965), paper 94.
33. Cheifetz, e., Gilat,J. Yavin,A.I. and Cohen, S.G., Phys. Letters 1 (1962) 289.
34. Macfarlane, R.D. and Almodovar, I.,Phys. Rev. 127 (1962) 1665.
35. Poortmans, F. and Ceulemans,H., De Ruyter,A.J. and Nève de Mévergnies,M., Nuclear Phys. 82 (1966) 331.
36. Dakowski, M., Krogulski,T., Piasecki,E., Piekarz,H. and Sowinski,M., Nuclear Phys. 97 (1967) 187.
37. Goldberg, M.D., Mughabghab, S.F., Purohit,S.N., Magurno,B.A. and May,V.M., B.N.L. 325, second edition 1966.
38. Popov, Yu,P. and Stempinskii,M., J.E.T.P. Letters 7 (1968) 97.
39. Blichert-Toft, P.H., Funk,E.G. and Mihelich,J.W., Nuclear Phys. 79 (1966) 12.
40. Smither, R.K., Phys. Letters 25B (1967) 128.
41. Church,E.L. and Wesener, J., Bull. Am. Phys. Soc. 13 (1968) 893.
42. Church, E.L. Private communication.
43. Draper, I.E. and Springer,T.E., Nuclear Phys. 16 (1960) 27.
44. Hansen, O. and Nathan,O., Nuclear Phys. 42 (1963) 197.
45. Fenner,N.C., Large, R.S. J. Inorg. Nucl. Chem. 29 (1967) 2147.
46. Whitten, R.N., A.A.E.C. report TM443 (1968).
47. Mattauch, J.H.E., Thiele,W. and Wapstra, A.H., Nuclear Phys. 67 (1965) 1.
48. Chiao,L.W., Nuclear Data Sheets 5-5-26 (1963).

CHAPTER VI

SOME REMARKS CONCERNING THE ENERGY LEVEL SCHEMES OF ^{144}Nd AND ^{150}Sm.

The collective nuclear model has been successfully used to describe the energy level schemes of nuclei which are far from closed shells. Such nuclei have a permanent ground state deformation. Many of their lowest energy levels correspond to rotational modes of the nuclear mass. In addition vibrational excitations of the nucleus can be observed. Even-even nuclei which are not far from closed shells are nearly spherical. Their lowest energy levels can often be considered as vibrational modes of the nuclear surface. In the regions $150 \lesssim A \lesssim 190$ and $A \gtrsim 220$, where A is the nuclear mass number, the nuclei have a permanent ground state deformation. Nearly spherical nuclei can be found in the regions $60 \lesssim A \lesssim 150$ and $190 \lesssim A \lesssim 220$.

The nucleus ^{144}Nd, which is nearly spherical, has only two neutrons outside a closed neutron shell. The lowest 2^+ level at 696 keV is generally assumed to be a one-phonon vibrational level; the transition probability to the ground state is enhanced by a factor of about 40 and it is below the energy of about 1.5 MeV necessary for a two-quasiparticle excitation of this nucleus [1,2]. The two-phonon vibrational levels with spins and parities 0^+, 2^+ and 4^+ are expected at about twice the energy of the first excited 2^+ level. The 4^+ and 2^+ levels, at 1314 and 1560 keV respectively, may be considered as such states. Yet there are various reasons to assume that they are to a large extent influenced by shell model effects:

a. The energy difference between the 4^+ and 2^+ levels is rather large and a 0^+ level has not been observed in the neighbourhood of these two levels.
b. The $2^{+'} \rightarrow 2^+$ transition is mainly of M1 character.

The systematics of one-phonon 2^+ states of a wide range of nuclei have been studied and compared with theoretical models by several authors [3,4]. The agreement is satisfactory generally speaking. For higher excitation energies, where particle and collective excitations are both possible, simple

predictions based on collective model calculations give poor results. In individual cases, reasonable agreement has sometimes be obtained with a collective model, modified by interparticle interactions, as has been used for instance by Raz[5]. He considered a spherical core with only two identical particles outside of a closed shell. The particles are coupled to each other by a simple two body interaction and they are coupled to the core. In this calculation, two particles in the $f_{\frac{7}{2}}$ shell were considered. Two parameters were introduced: D, which is a measure of the strength of the interaction between the two extra nucleons, and x denoting the particle surface coupling. Calculations similar to those made by Raz have more recently been performed by Heyde and Brussaard [6]. Instead of D and x they have used slightly differently defined paramaters (G and ξ). The 'one-phonon' 2^+ level at 696 keV, the 4^+ and $2^{+'}$ 'two phonon' levels at 1314 and 1560 keV and the 6^+ level at 1791 keV [7], which was assumed to be a 'three-phonon' level, fit the theoretical predictions fairly well if D=0.8 and x=0.25 are used (or G=0.65 and ξ=1.5 in ref. 5). The energies calculated in ref. 6 for the parameter values given above (and the experimental values between parentheses) for these levels are as follows: 696(696)2^+, 1384(1314)4^+, 1509(1560)$2^{+'}$ and 1742(1791)6^+. The first excited 0^+ state is shifted in both calculations to much higher energies. In ref. 5 the $0^{+'}$ level is expected at 2063 keV. Recently a level with spin 0 was observed [8] at 2085 keV which consequently might be a member of the 'three-phonon triplet'.

A further comparison between the model calculations just mentioned and experimental data is possible by considering the reduced intensities and also the M1-E2 mixing ratio of the $2^{+'} \rightarrow 2^+$ transition. The ratio B(E2; $2^{+'} \rightarrow 0^+$)/B(E2;$2^{+'} \rightarrow 2^+$) of the reduced intensities, which can be estimated with the data given in ref. 7 to be less than 0.001, can only be understood by assuming exceptional values of the parameters. The experimentally determined mixing ratio δ of the $2^{+'} \rightarrow 2^+$ transition is of the same order of magnitude as the δ calculated by Raz[5] (calculated value of Raz is $|\delta| = 0.24$; experimental value is $0.45 < |\delta| < 0.65$). The agreement with the more recent calculations of Heyde and Brussaard seems to be less favorable ($|\delta| = 0.05$).
In general both calculations show the possibility of appreciable M1 matrix elements for the $2^{+'} \rightarrow 2^+$ transition.

Attempts to describe the energy level scheme of ^{150}Sm with simple models have met with little success. This can be attributed to the fact that

it is in a transition region between clearly spherical and deformed nuclei. It has been suggested by Sheline[9] that there is a relation between energy levels of even-even nuclei in the spherical and deformed regions: Going from the spherical to the deformed region the 0^+ and 2^+ states of the two-phonon triplet in spherical nuclei gradually tend to the β - and γ-vibrational states in deformed nuclei while the 4^+ state of this triplet corresponds to the 4^+ rotational state in the ground-state band of the deformed nuclei. Attempts have been made to verify this suggestion and it seems that the general trend in the energy levels mentioned above is observed in the even samarium nuclei[10].

It is interesting to compare the detailed level scheme of ^{150}Sm with the latest published information of neighbouring even-even nuclei in order to see whether it is possible to find correlations between the different level schemes. The energy levels of ^{148}Sm, ^{150}Sm and ^{152}Sm are collected in fig. 6.1. Of these nuclei, ^{152}Sm apparently is a strongly deformed nucleus in which rotational bands are clearly observed while ^{148}Sm is a nearly spherical nucleus. In addition, levels of ^{152}Gd, which is expected to have a level scheme similar to the level scheme of ^{150}Sm, are given. Parentheses around a spin value mean that the spin and parity assignments are uncertain. A bar over a spin value means that other levels were observed near the corresponding level which have or may have the same spin and parity. The data of ^{148}Sm have been taken from ref. 11-14. Below 1680 keV no more energy levels have been observed in ^{148}Sm, than those indicated in fig. 6.1. All levels which have been observed in ^{150}Sm below 1650 keV are reproduced in fig. 6.1. The data of ^{152}Sm were taken from ref. 12-17. The levels observed in ^{152}Gd below 1470 keV are given in fig. 6.1 except the 1^- level at 1315 keV. The experimental data were taken from ref. 12-14 and 16-18.

The levels of the nuclei mentioned above which correspond to the ground state rotational band in strongly deformed nuclei with spins and parities 0^+, 2^+, 4^+, 6^+,... are shown at the left hand side in fig. 6.1. The second 0^+ state of each nucleus is supposed to be a β-vibration. The rotational states with spins and parities 2^+, 4^+, ... built on to this β-vibration were found, using the assumptions that the spacing between the energy levels is about the same as in the ground state band and that E2 transitions between the successive members of the band do exist. The next 2^+ states were assumed to be γ-vibrations. The lowest 3^+ state was supposed to be the first rotational

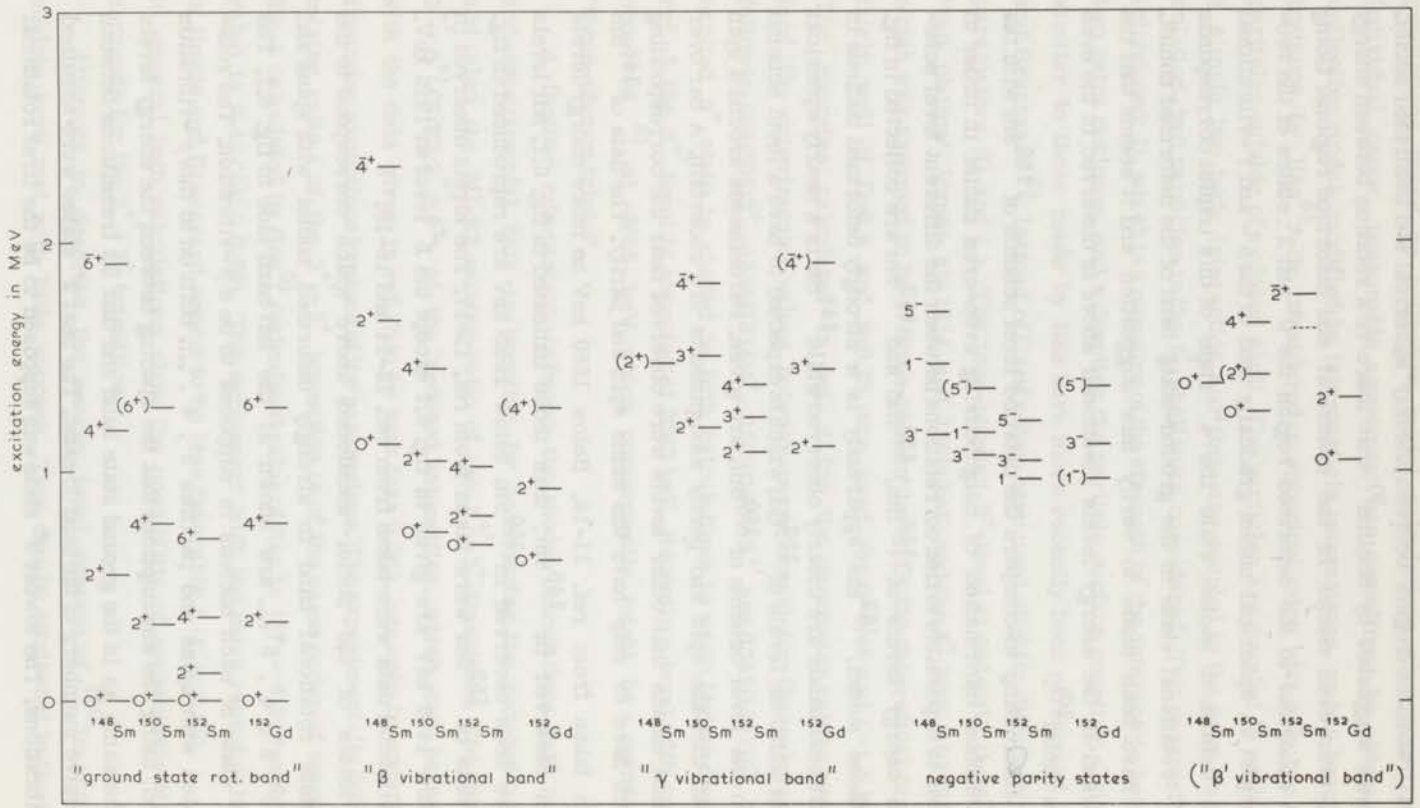

Fig. 6.1 Comparison of the energy levels of ^{150}Sm with neighbouring even-even samarium nuclei and with ^{152}Gd.

state built onto the γ-vibration. For each nucleus three of the lowest negative parity states with spins 1, 3 and 5 are also given in fig. 6.1. A general trend in the levels with equal spin can be observed. After arranging the energy levels in the way mentioned above three levels below 1650 keV with a spin and parity sequence 0^+, 2^+, 4^+ remained unidentified in the level scheme of ^{150}Sm. This triad of levels may belong to a band built onto a second β-vibration. In order to find corresponding bands in the other nuclei we looked for the third 0^+ states and fourth 2^+ states. These bands are possibly present in the other samarium nuclei but at somewhat higher energies.

The energy level schemes of ^{150}Sm and ^{152}Gd are similar. The energies of the β- and γ-vibrations are somewhat lower in ^{152}Gd, but the spacing between the energy levels in the corresponding bands is about the same.

Finally it may be remarked that the observed transitions without parity change and $\Delta I = 0, \pm 1$ between the levels of ^{150}Sm which are given in fig. 6.1, generally have E2 character. Thus all experimentally observed energy levels of ^{150}Sm up to 1650 keV appear to have collective characteristics.

REFERENCES

1. Gilbert,A. and Cameron,A.G.W., Can. J. Phys. 43 (1965)1446.
2. Fulmer, R.H., McGarthy, A.L. and Cohen, B.L., Phys. Rev. 128 (1962) 1302.
3. Nathan, O. and Nilsson S.G., Alpha- Beta- and Gamma-ray spectroscopy, Vol. 1, Chapter X (1965).
4. Kisslinger,L.S. and Sorensen,R.A., Rev. of Mod. Phys. 35 (1963) 853.
5. Raz,B.J., Phys. Rev. 114 (1959) 1116 and Phys. Rev. 129 (1963) 2622.
6. Heyde,K., Brussaard,P.J., Nuclear Phys. 104 (1967) 81.
7. Raman,S., Nuclear Data Sheets B2-1-47 (1967).
8. Raman,S., Nuclear Phys. 107 (1968) 402.
9. Sheline,R.K., Rev. Mod.Phys. 32 (1960) 1.
10. Sakai,M., Nuclear Phys. 104 (1967) 301.
11. Martin,M.J., Nuclear Data Sheets B2-4-79 (1967).
12. Keddy,R.J., Yoshizawa,Y., Elbek,B., Herskind, B. and Olesen, M.C., Nuclear Phys. 113 (1968) 676.
13. Veje, E., Elbek, B., Herskind, B. and Olesen, M.C., Nuclear Phys.109 (1968) 489.
14. Morinaga,H., Nuclear Phys. 75 (1966) 385.
15. Ishizaki,Y., Sasaki,K. and Yoshida,Y., Report JAERI 1158 (1968) 47.
16. Dzhelepov, B.S., Zhukovskii, N.N. and Maloyan, A.G., Sov. J.Nuclear Phys. 3 (1966) 577.
17. Larsen,J.S., Skilbreid,O. and Vistisen,L., Nuclear Phys. 100 (1967) 248.
18. Seaman,G.G., Greenberg,J.S. Bromley,D.A. and McGowan,F.K., Phys. Rev. 149 (1966) 925.

SAMENVATTING

De in dit proefschrift beschreven experimenten werden uitgevoerd bij de hoge flux reactor in Petten. Neutronenbundels van deze reactor werden gebruikt om de gammastraling te bestuderen die van kernen na vangst van langzamen neutronen uitgaat. Op deze wijze kan men informatie verkrijgen over de vervalschema's van de resulterende samengestelde kernen. Voor een vergelijking met kernmodellen zijn ook de spins en pariteiten van de energieniveaus van belang. Deze werden bepaald door van gerichte (gealigneerde) kernen de anisotropie in de hoekverdeling en de lineaire polarisatie van de gammastraling te meten. De kernen ^{143}Nd en ^{149}Sm kunnen worden gericht in eenkristallen van respectievelijk neodymiumethylsulfaat en cerium (samarium)magnesium dubbelnitraat door deze af te koelen tot een temperatuur van ongeveer 0.01 K. Deze lage temperatuur werd verkregen met behulp van de methode van de adiabatische demagnetisatie. De preparaten voor de anisotropiemetingen werden vervaardigd met behulp van natuurlijk neodymium en natuurlijk samarium. Daar beide elementen meerdere stabiele isotopen bevatten die allen kunnen bijdragen tot de neutronenvangst gammaspectra werden in een afzonderlijk experiment gammaspectra opgenomen van preparaten, die verrijkt zijn in een enkel isotoop om na te gaan welke gammaovergangen bij welk isotoop behoren. Op deze wijze kon nog enige informatie worden ingewonnen over de vervalschema's van ^{146}Nd, ^{148}Sm en ^{153}Sm. In hoofdstuk II wordt een overzicht gegeven van de formules, die de afhankelijkheid van de hoekverdeling en de lineaire polarisatie van de spins en pariteiten van de energieniveaus en de multipoolmengingen in de gamma-overgangen beschrijven. De gebruikte apparatuur, bestaande uit cryostaat, magneet voor adiabatische demagnetisatie, Ge(Li)detectoren, electronica en de gebruikte neutronenbundels worden beschreven in hoofdstuk III. De experimentele resultaten voor de neodymium en samarium kernen worden besproken in de hoofdstukken IV en V. Verschillende spins en pariteiten van energieniveaus in ^{144}Nd en ^{150}Sm werden bepaald.

Tenslotte worden in Hoofdstuk VI nog enkele opmerkingen gemaakt over de energieniveauschema's van de onderzochte kernen.

Teneinde te voldoen aan de wens van de Faculteit der Wiskunde en Natuurwetenschappen volgen hier enkele persoonlijke gegevens.

In 1953 behaalde ik het einddiploma B aan de Oldenbarnevelt H.B.S. te Rotterdam. In dat zelfde jaar begon ik mijn studie aan de Rijksuniversiteit te Leiden. Het kandidaats examen a werd in 1957 afgelegd. In 1960 volgde het doctoraal examen experimentele natuurkunde met als bijvak wiskunde. De vereiste tentamens werden afgelegd bij Prof. Dr S.R.de Groot, Dr J.van Kranendonk, Dr P.Mazur, Prof. Dr C.Visser en Ir J.Snijder. Van 1960 tot 1965 was ik als leraar verbonden aan de Rijks H.B.S. te Gorinchem.

Mijn praktische opleiding begon in het Kamerlingh Onnes Laboratorium bij de afdeling paramagnetische relaxatie waar ik samenwerkte met J.C. Verstelle en P.R.Locher. In 1965 trad ik in dienst van de Stichting F.O.M. bij de groep voor kernorientatie te Petten.

Tijdens het onderzoek te Petten ondervond ik zeer veel steun van Dr H.Postma die steeds bereid was mij met raad en daad bij te staan. De heren K.Ravensberg en J.J.Smit hebben door hun technische werkzaamheden veel bijgedragen tot het slagen van de experimenten. Tijdens de metingen en voor het uitwerken van de gegevens werd ik van tijd tot tijd bijgestaan door de heren J.F.M.Potters en R.Kuiken. De samenwerking met veel van de medewerkers van het Reactor Centrum werd zeer gewaardeerd. De tekeningen in dit proefschrift werden grotendeels verzorgd door de heer F.Tegelaar. Veel van het typewerk werd gedaan door Mej. G.Möls.